Cell Reports
Medicine

Article

AAV-mediated gene therapy produces fertile offspring in the *Lhcgr*-deficient mouse model of Leydig cell failure

Graphical abstract

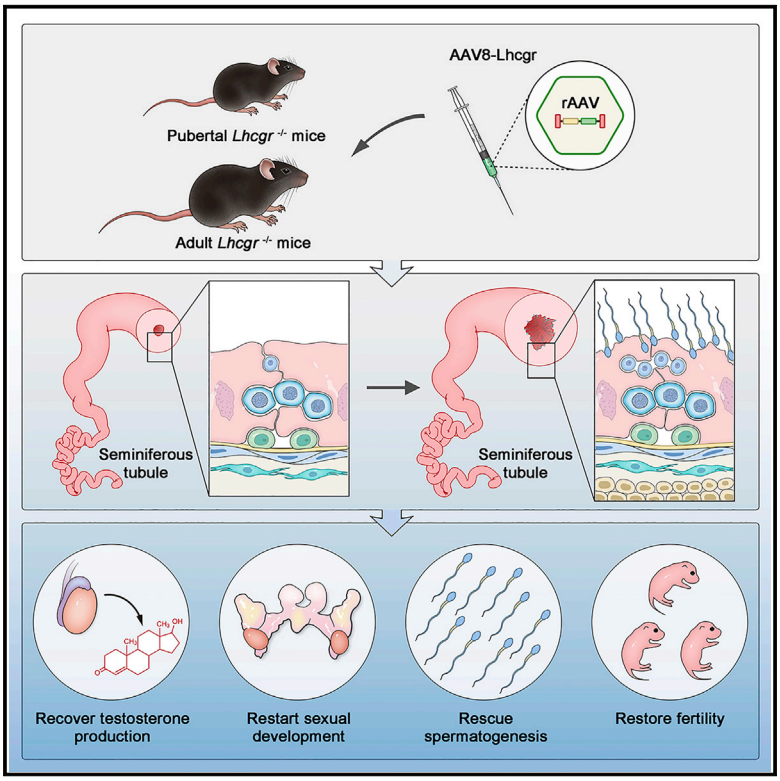

Highlights

- AAV8 targets progenitor Leydig cells through interstitial injection in the testes
- AAV8-Lhcgr partially increases testosterone production and initiates sexual development
- AAV8-Lhcgr recovers spermatogenesis and effectively produces fertile offspring
- These favorable therapeutic effects could be reproduced in adult male *Lhcgr*$^{-/-}$ mice

Authors

Kai Xia, Fulin Wang, Xingqiang Lai, ..., Frank Fuxiang Mao, Chunhua Deng, Andy Peng Xiang

Correspondence

dengchh@mail.sysu.edu.cn (C.D.), xiangp@mail.sysu.edu.cn (A.P.X.)

In brief

Leydig cell failure results in testosterone deficiency and male infertility. Xia et al. demonstrate AAV-mediated gene therapy recovers testosterone levels, restarts sexual development, restores spermatogenesis, and produces fertile offspring in a mouse model of Leydig cell failure, and thus may have value for future clinical applications.

Xia et al., 2022, Cell Reports Medicine *3*, 100792
November 15, 2022
https://doi.org/10.1016/j.xcrm.2022.100792

CellPress

Cell Reports Medicine

CellPress
OPEN ACCESS

Article

AAV-mediated gene therapy produces fertile offspring in the *Lhcgr*-deficient mouse model of Leydig cell failure

Kai Xia,[1,2,6,7] Fulin Wang,[1,2,7] Xingqiang Lai,[3,7] Lin Dong,[2,7] Peng Luo,[1,2] Suyuan Zhang,[2] Cuifeng Yang,[1,2] Hong Chen,[2] Yuanchen Ma,[2] Weijun Huang,[2] Wangsheng Ou,[4] Yuyan Li,[1] Xin Feng,[1,2] Bin Yang,[2] Congyuan Liu,[2] Zhenmin Lei,[5] Xiang'an Tu,[1] Qiong Ke,[2] Frank Fuxiang Mao,[4] Chunhua Deng,[1,*] and Andy Peng Xiang[2,6,8,*]

[1]Department of Urology and Andrology, The First Affiliated Hospital, Sun Yat-sen University, Guangzhou, Guangdong 510080, China
[2]Center for Stem Cell Biology and Tissue Engineering, Key Laboratory for Stem Cells and Tissue Engineering, Ministry of Education, Sun Yat-sen University, Guangzhou, Guangdong 510080, China
[3]Cardiovascular Department, The Eighth Affiliated Hospital, Sun Yat-sen University, Shenzhen, Guangdong 518033, China
[4]State Key Laboratory of Ophthalmology, Zhong Shan Ophthalmic Center, Sun Yat-sen University, Guangzhou, Guangdong 510000, China
[5]Department of OB/GYN and Women's Health, University of Louisville School of Medicine, Louisville, KY 40292, USA
[6]National-Local Joint Engineering Research Center for Stem Cells and Regenerative Medicine, Zhongshan School of Medicine, Sun Yat-sen University, Guangzhou, Guangdong 510080, China
[7]These authors contributed equally
[8]Lead contact
*Correspondence: dengchh@mail.sysu.edu.cn (C.D.), xiangp@mail.sysu.edu.cn (A.P.X.)
https://doi.org/10.1016/j.xcrm.2022.100792

SUMMARY

Leydig cell failure (LCF) caused by gene mutation results in testosterone deficiency and infertility. Serum testosterone levels can be recovered via testosterone replacement; however, established therapies have shown limited success in restoring fertility. Here, we use a luteinizing hormone/choriogonadotrophin receptor (*Lhcgr*)-deficient mouse model of LCF to investigate the feasibility of gene therapy for restoring testosterone production and fertility. We screen several adeno-associated virus (AAV) serotypes and identify AAV8 as an efficient vector to drive exogenous *Lhcgr* expression in progenitor Leydig cells through interstitial injection. We observe considerable testosterone recovery and Leydig cell maturation after AAV8-Lhcgr treatment in pubertal $Lhcgr^{-/-}$ mice. Of note, this gene therapy partially recovers sexual development, substantially restores spermatogenesis, and effectively produces fertile offspring. Furthermore, these favorable effects can be reproduced in adult $Lhcgr^{-/-}$ mice. Our proof-of-concept experiments in the mouse model demonstrate that AAV-mediated gene therapy may represent a promising therapeutic approach for patients with LCF.

INTRODUCTION

Testosterone is the key hormone that regulates the development and maintenance of the masculine phenotype and reproductive function.[1] Leydig cells, located in the interstitial compartment of the testis and nestled among the seminiferous tubules, are primarily responsible for the production of testosterone via a multistep process involving multiple genes.[2] When one of these genes is deficient, Leydig cell failure (LCF) occurs; this causes testosterone deficiency, which further contributes to arrested spermatogenesis and infertility.[3,4] In such cases, serum testosterone levels can be normalized through testosterone replacement therapy (TRT).[5] However, infertility is almost always present in patients with genetic LCF, and conventional established therapies have shown limited success in addressing this issue.[6,7] Thus, there is a significant need for ideal approaches to treat genetic LCF.

Given that the underlying cause of poor testosterone production in LCF is a genetic variant in a gene involved in regulating steroidogenic pathways,[4] gene therapy is considered one of the most promising potential therapeutic strategies. In previous studies, transduction of genes into the testis has been achieved by microinjection of lentiviruses or adenoviruses.[8–10] However, adenovirus induces an inflammatory reaction in the testis and its expression gradually lost.[8,10,11] Moreover, lentivirus can transduce genes into germ cells, including SSCs,[9] which causes ethical concerns. Among the available gene delivery vectors, recombinant adeno-associated virus (AAV) vectors have become a powerful tool for *in vivo* gene therapy due to their desirable safety profile.[12] In the past few years, AAV-mediated gene therapies have been applied to treat many genetic defects, such as those involved in hemophilia,[13] muscle diseases,[14] brain disorders,[15] retinitis pigmentosa,[16] and deafness.[17] However, whether AAV-mediated gene delivery could be used to restore testosterone production and benefit fertility in genetic LCF remains unknown. Thus, there is an urgent demand to investigate the feasibility of AAV-mediated gene therapy in an animal model of genetic LCF.

Previous reports have described a mouse model of hereditary LCF, which occurs as a result of a null mutation in the gene encoding luteinizing hormone/choriogonadotrophin receptor (*Lhcgr*).[18,19] As a highly conserved gene among mammalian species, *Lhcgr* plays important roles in reproduction.[20] More specifically, *Lhcgr* is required for the maturation of Leydig cells and the synthesis of testosterone, which regulates the development of sex organs and promotes spermatogenesis.[20] In $Lhcgr^{-/-}$ male mice, the development of Leydig cells is impaired, which leads to a dramatic reduction in testosterone levels.[18,19] Additionally, $Lhcgr^{-/-}$ male mice exhibit stunted sexual development, defective spermatogenesis, and infertility.[18,19] Mice homozygous for the mutation mimic the phenotype of LCF in humans,[21] and thus serve as an excellent animal model for gene delivery studies.

Here, we used the *Lhcgr*-deficient mouse model of LCF to investigate whether AAV-mediated gene therapy can restore Leydig cell function and restart sexual development in pubertal mice. We subsequently elucidated whether this gene therapy could rescue spermatogenesis and the production of fertile offspring. Furthermore, we investigated the therapeutic effect in adult mice to determine the therapeutic potential of this gene therapy in adult patients who had missed puberty. Finally, we examined the feasibility and translational potential of gene therapy in pubertal male cynomolgus monkeys.

RESULTS

Testicular injection of AAV8 targets progenitor Leydig cells

Several previous studies suggested that Leydig cell differentiation is blocked in the progenitor cell stage in the postnatal testis of *Lhcgr*-deficient LCF mice.[19,22] Because different AAV serotypes have shown distinct tissue or cell tropisms, to identify the AAV serotypes with the highest viral transduction rate toward progenitor Leydig cells, we interstitially injected AAV-CAG-mCherry reporter vectors containing the commonly used AAV serotypes 1, 2, 6, 8, or 9 at titers of 8×10^{10} genome copies (gc) into each testis of $Lhcgr^{-/-}$ mice. We performed histological analysis of the testes 7 days after vector injection and found that, at equivalent viral titers, AAV8 exhibited the highest efficiency among the tested serotypes, as demonstrated by co-expression of mCherry and the progenitor Leydig cell markers Nestin and platelet-derived growth factor receptor α (PDGFRα) (Figures S1A and S1B). AAV8 successfully transduced over 80% progenitor Leydig cells on average in the interstitium of the testes (Figures S1C and S1D). Thereafter, we evaluated the tropism of AAV8 for germ cells and Sertoli cells. Immunostaining analysis revealed that mCherry was not co-expressed with the germ cell marker DEAD-box helicase 4 (DDX4) or the Sertoli cell marker SRY-box transcription factor 9 (SOX9), indicating the absence of AAV infection in these two cell types (Figure S1E). We also performed immunostaining experiments to detect the co-expression pattern of AAV8-mCherry with the peritubular myoid cell marker alpha-smooth muscle actin (α-SMA) and macrophage marker allograft inflammatory factor 1 (AIF1) and revealed that mCherry was minimally co-expressed with a-SMA or AIF1, indicating a remote chance of AAV8 infection in these two cell types (Figure S1E). These results indicate that the interstitial injection of AAV8 could effectively target progenitor Leydig cells in $Lhcgr^{-/-}$ mice.

Moreover, we performed experiments to evaluate the possibility of the off-target transduction in other tissues. Immunofluorescence analysis revealed that mCherry was expressed in the testis but not in the liver, heart, muscle, kidney, or colon (Figure S2A), indicating that AAV8 showed a clear testis tropism when injected interstitially into the testis. Quantitative RT-PCR analysis of testicular tissue showed that the administration of AAV8-mCherry resulted in transiently increased transcripts of key inflammatory genes in testes at day 1 and day 3, whereas the expression level of these genes returned to normal level within 7 days (Figure S2B). We further examined the infiltration of $CD4^+$ and $CD8^+$ lymphocytes 7 days after AAV8-mCherry injection and there was no significant difference in lymphocyte infiltration between the two groups with or without injection (Figure S2C). These results suggest that interstitial injection of AAV8 is safe and well tolerated.

Gene delivery of AAV8-Lhcgr increases *Lhcgr* expression in the testes and recovers testosterone levels in pubertal $Lhcgr^{-/-}$ mice

Next, we used an established $Lhcgr^{-/-}$ mouse model of LCF to determine whether AAV-based gene therapy could be efficacious in recovering *Lhcgr* expression and testosterone levels. We generated AAV8 vectors that carried the coding sequence of mouse *Lhcgr* with the CAG promoter (AAV8-Lhcgr), which were used in subsequent experiments (Figure 1A). To evaluate the functionality of these vectors, we first chose pubertal $Lhcgr^{-/-}$ mice (3 weeks old) to determine the potential therapeutic effects of this gene therapy in LCF patients at puberty (Figure 1B). These mice were interstitially injected with phosphate-buffered saline (PBS) or AAV8-Lhcgr at doses of 8×10^9, 4×10^{10}, 8×10^{10}, or 2×10^{11} gc/testis. Sham-operated littermate $Lhcgr^{+/+}$ and $Lhcgr^{+/-}$ mice served as controls. To evaluate gene transfer efficiency, we measured the RNA transcript and protein levels of *Lhcgr* at 4 weeks after AAV8-Lhcgr administration. Quantitative RT-PCR analysis of testicular tissue showed that AAV8-Lhcgr resulted in dose-dependent expression of *Lhcgr* transcripts in testes from injected $Lhcgr^{-/-}$ mice, whereas *Lhcgr* expression was not detectable in $Lhcgr^{-/-}$ mice treated with PBS (Figure 1C). Accordingly, immunostaining demonstrated obvious LHCGR expression in the testicular interstitium in the AAV8-Lhcgr-treated group (8×10^{10} gc/testis), whereas LHCGR was negligibly detected in the testes from $Lhcgr^{-/-}$ mice treated with PBS (Figure 1D).

In addition, serum testosterone concentrations were significantly and dose-dependently increased in $Lhcgr^{-/-}$ mice treated with AAV8-Lhcgr compared with PBS (Figure 1E). Serum testosterone levels in mice treated with 8×10^{10} and 2×10^{11} gc/testis of AAV8-Lhcgr reached approximately 30% of the levels observed in $Lhcgr^{+/+}$ or $Lhcgr^{+/-}$ mice, whereas the level was profoundly lower (nearly undetectable) in PBS-treated $Lhcgr^{-/-}$ mice (Figure 1E). Notably, the concentration of intratesticular testosterone, which is vital for spermatogenesis,[6] was also increased in AAV8-Lhcgr-treated mice (8×10^{10} gc/testis) compared with those in the PBS-treated group at 4 weeks after

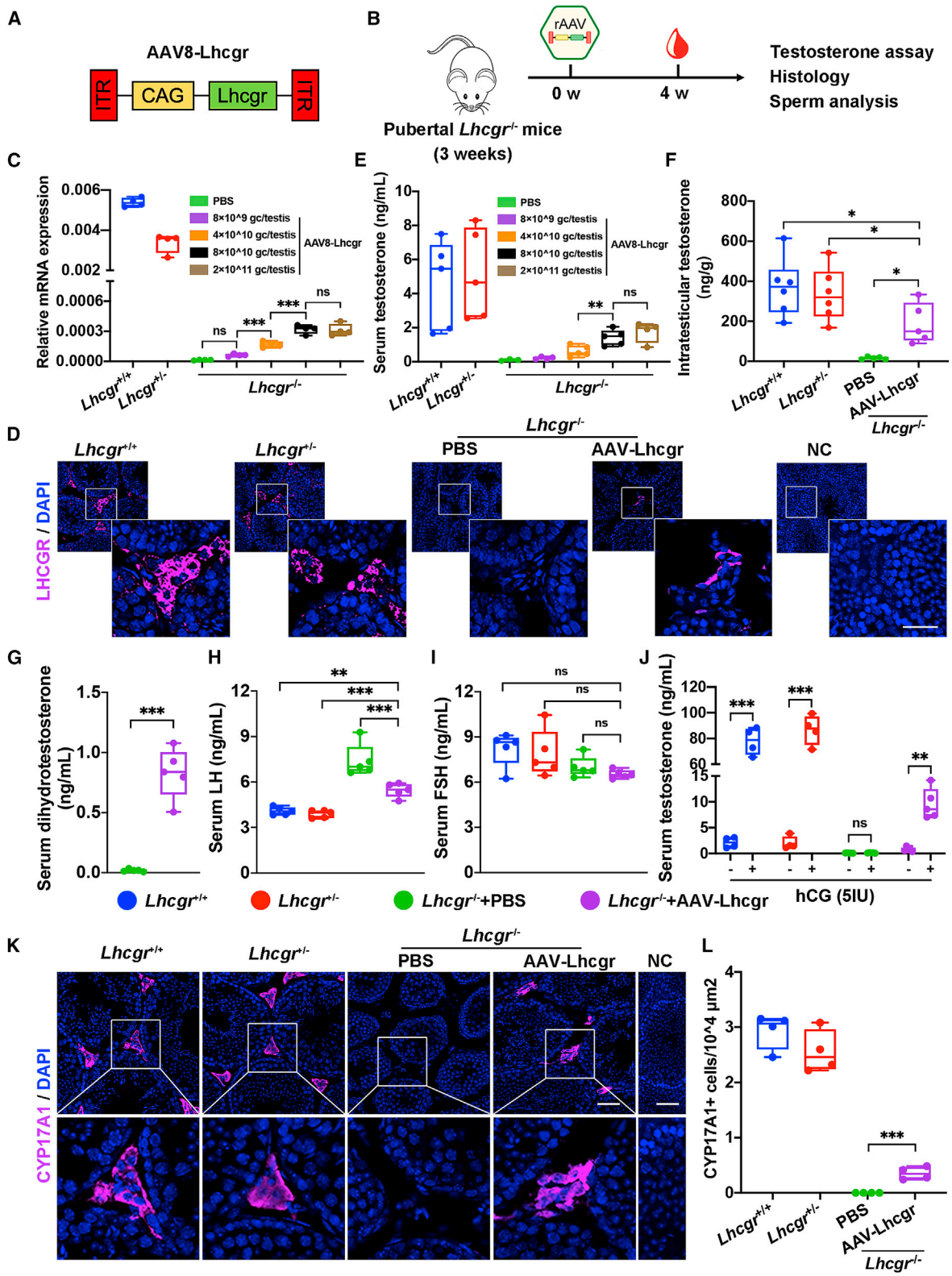

(legend on next page)

treatment (Figure 1F). Serum dihydrotestosterone concentrations were significantly increased in *Lhcgr*$^{-/-}$ mice treated with AAV8-Lhcgr compared with PBS in the pubertal cohort 4 weeks post treatment (Figure 1G). These results confirm that AAV-mediated gene therapy recovers testosterone production. We further measured serum luteinizing hormone (LH) and follicle-stimulating hormone (FSH) levels in the pubertal cohort. As expected, LH levels decreased significantly 4 weeks after AAV8-Lhcgr injection (Figure 1H). We did not observe significant changes in FSH levels (Figure 1I). These results reflect the normal negative feedback effect of hypothalamic-pituitary-gonad axes on testosterone levels.

To assess the impact of gene therapy on Leydig cell maturation in the pubertal cohort, we injected mice from four groups with human chorionic gonadotropin (hCG) to assess the function of Leydig cells. Consistent with the results observed in *Lhcgr*$^{+/+}$ or *Lhcgr*$^{+/-}$ mice, serum testosterone concentrations increased more than 10 times after hCG injection in *Lhcgr*$^{-/-}$ mice treated with AAV8-Lhcgr (Figure 1J). However, serum testosterone levels remained profoundly lower before and 1 h after hCG injection in PBS-treated *Lhcgr*$^{-/-}$ mice (Figure 1J). We next examined the expression levels of the mature Leydig cell marker cytochrome P450 family 17 subfamily A member 1 (CYP17A1) in testes 4 weeks after AAV8-Lhcgr injection. Immunofluorescence analysis showed partially increased CYP17A1^{+} Leydig cell numbers in AAV-treated *Lhcgr*$^{-/-}$ mice compared with PBS-treated mice in the interstitial space of testes samples (Figures 1K and 1L). These data suggest that AAV8-Lhcgr treatment in pubertal *Lhcgr*$^{-/-}$ mice promoted Leydig cell maturation.

AAV8-Lhcgr restarts sexual development in pubertal *Lhcgr*$^{-/-}$ mice

Based on the observation that testosterone levels and the maturation of Leydig cells from *Lhcgr*$^{-/-}$ mice were promoted after AAV8-Lhcgr therapy (8×10^{10} gc/testis), we next examined whether these features were accompanied by normalization of sexual development. Intriguingly, in *Lhcgr*$^{-/-}$ mice treated with AAV8-Lhcgr, we found that the retained testes descended into the scrotum 4 weeks after gene delivery. Moreover, the underdeveloped external genitals (penis and scrotum) of the *Lhcgr*$^{-/-}$ mice approached the size of those observed in *Lhcgr*$^{+/+}$ and *Lhcgr*$^{+/-}$ mice (Figures 2A and 2B).

Further examination revealed that the ano-genital distances were increased in AAV8-Lhcgr-treated *Lhcgr*$^{-/-}$ mice compared with the PBS-treated group (Figure 2C), indicating that masculinization was promoted after gene therapy. AAV8-Lhcgr treatment also increased penile length compared with that of PBS-treated *Lhcgr*$^{-/-}$ mice (Figure 2D). The testis weights of AAV8-Lhcgr-treated mice were approaching the level of those in *Lhcgr*$^{+/+}$ or *Lhcgr*$^{+/-}$ mice, whereas testis weights in the PBS-treated group remained considerably lower (Figure 2E). In addition, the hypoplastic epididymis of *Lhcgr*$^{-/-}$ mice grew markedly under AAV8-Lhcgr treatment, almost reaching the size observed in *Lhcgr*$^{+/+}$ and *Lhcgr*$^{+/-}$ mice (Figure 2F). The seminal vesicle weight, which is a well-established biomarker of androgen exposure,[23] increased in the AAV8-Lhcgr group to approximately 37% of the weights in *Lhcgr*$^{+/+}$ and *Lhcgr*$^{+/-}$ mice, whereas the seminal vesicles were macroscopically undetectable in PBS-treated *Lhcgr*$^{-/-}$ mice (Figure 2G). The prostates of AAV8-Lhcgr-treated *Lhcgr*$^{-/-}$ mice weighed more than those of the PBS-treated group and were more than half of the prostate weight in *Lhcgr*$^{+/+}$ and *Lhcgr*$^{+/-}$ mice (Figure 2H). The weight and length of the vas deferens were increased in AAV8-Lhcgr-treated *Lhcgr*$^{-/-}$ mice compared with PBS-treated group, although these parameters remained significantly lower than those recorded in the *Lhcgr*$^{+/+}$ and *Lhcgr*$^{+/-}$ groups (Figure 2I and 2J). Overall, these results strongly support the notion that AAV8-Lhcgr restarts sexual development in pubertal *Lhcgr*$^{-/-}$ mice.

AAV8-Lhcgr rescues spermatogenesis in pubertal *Lhcgr*$^{-/-}$ mice

Given that AAV8-Lhcgr treatment could recover testosterone levels and promote sexual development in pubertal *Lhcgr*$^{-/-}$ mice, we next investigated whether AAV8-Lhcgr could rescue spermatogenesis. Histological analysis of the PBS-injected *Lhcgr*$^{-/-}$ testes showed that the seminiferous tubules were decreased in size and that spermatogenesis was arrested without any mature spermatozoa, as reported previously.[18,19]

Figure 1. Testicular injection of AAV8-Lhcgr rescues Leydig cell function and recovers testosterone levels in pubertal *Lhcgr*$^{-/-}$ mice

(A) Schematic of the AAV vector used in the study.

(B) Experimental overview of the *in vivo* studies.

(C) Quantitative RT-PCR was used to quantify *Lhcgr* mRNA transcripts in testicular tissues from *Lhcgr*$^{+/+}$ mice, *Lhcgr*$^{+/-}$ mice, and *Lhcgr*$^{-/-}$ mice injected with PBS or increasing doses of AAV8-Lhcgr (n = 4). β-actin was used for normalization.

(D) Representative images of LHCGR in the testes of *Lhcgr*$^{+/+}$ mice, *Lhcgr*$^{+/-}$ mice, and *Lhcgr*$^{-/-}$ mice injected with PBS or AAV8-Lhcgr (n = 4). Nuclei were counterstained with DAPI. NC, negative control. Scale bar: 25 μm.

(E) The concentrations of serum testosterone were analyzed in *Lhcgr*$^{+/+}$ mice (n = 5), *Lhcgr*$^{+/-}$ mice (n = 5), and *Lhcgr*$^{-/-}$ mice injected with PBS (n = 3) or increasing doses of AAV8-Lhcgr (8×10^{9} gc/testis [n = 4], 4×10^{10} gc/testis [n = 5], 8×10^{10} gc/testis [n = 5], and 2×10^{11} gc/testis [n = 4]).

(F) The concentrations of intratesticular testosterone were detected in *Lhcgr*$^{+/+}$ mice (n = 6), *Lhcgr*$^{+/-}$ mice (n = 6), and *Lhcgr*$^{-/-}$ mice injected with PBS (n = 5) or AAV8-Lhcgr (n = 5).

(G) The concentrations of serum dihydrotestosterone testosterone were analyzed in *Lhcgr*$^{-/-}$ mice injected with PBS or AAV8-Lhcgr (n = 5).

(H and I) The concentrations of serum LH (H) and FSH (I) were analyzed in *Lhcgr*$^{+/+}$ mice, *Lhcgr*$^{+/-}$ mice, and *Lhcgr*$^{-/-}$ mice injected with PBS or AAV8-Lhcgr (n = 5).

(J) The concentrations of serum testosterone were analyzed before and 1 h after hCG injection in *Lhcgr*$^{+/+}$ mice (n = 4), *Lhcgr*$^{+/-}$ mice (n = 4), and *Lhcgr*$^{-/-}$ mice injected with PBS (n = 5) or AAV8-Lhcgr (n = 5).

(K) CYP17A1 was evaluated by immunostaining of testes from *Lhcgr*$^{+/+}$ mice, *Lhcgr*$^{+/-}$ mice, and *Lhcgr*$^{-/-}$ mice injected with PBS or AAV8-Lhcgr (n = 4). NC indicates negative control. Scale bar: 50 μm.

(L) CYP17A1^{+} cells were quantified in the different groups. Data are represented by boxplots, and whiskers show the minimum to maximum values. *$p < 0.05$; **$p < 0.01$; ***$p < 0.001$; ns, not significant.

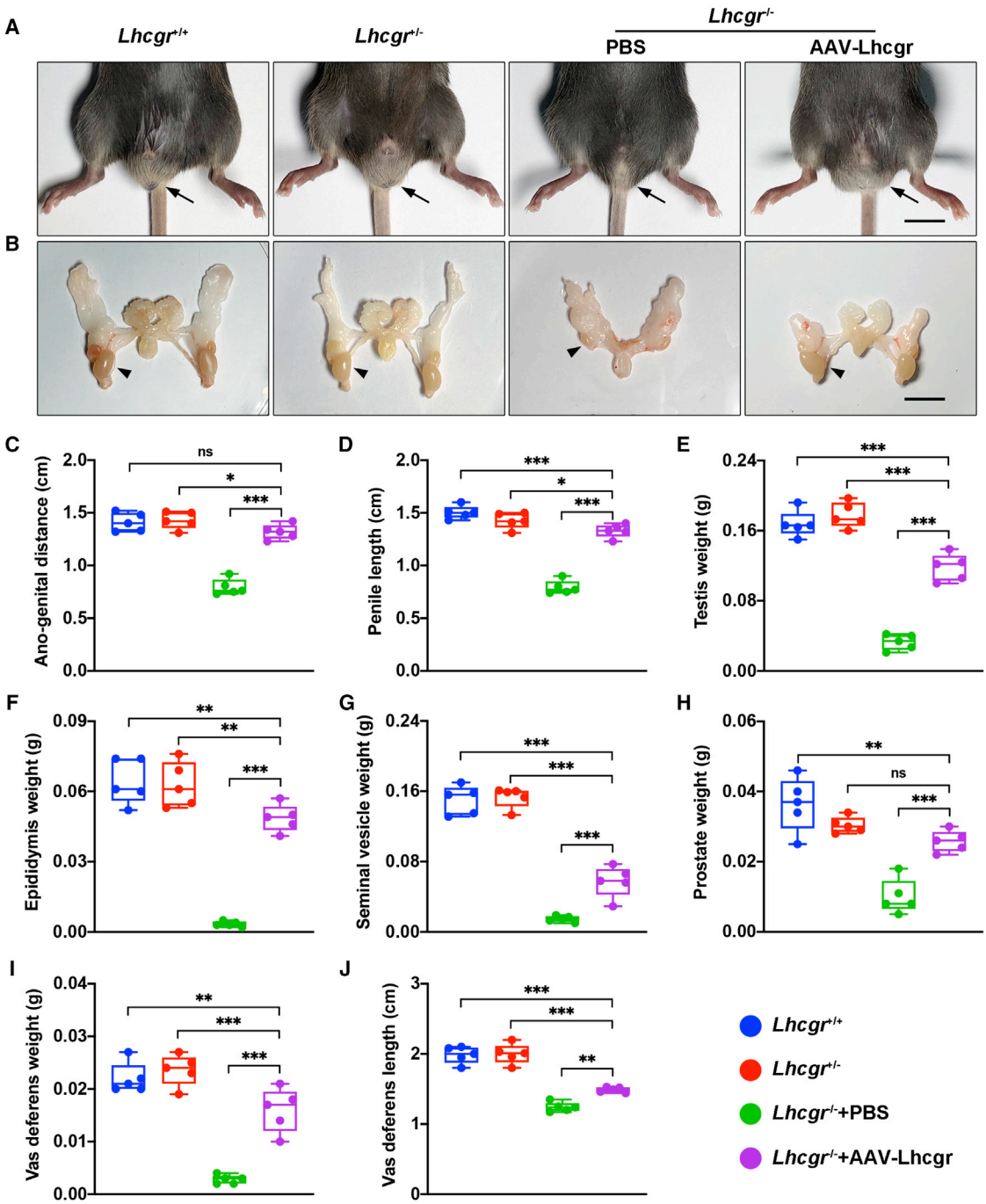

Figure 2. AAV8-Lhcgr restarts sexual development in pubertal *Lhcgr*$^{-/-}$ mice

(A and B) Representative photographs of the external (A) and internal genitalia (B) of *Lhcgr*$^{+/+}$ mice, *Lhcgr*$^{+/-}$ mice, and *Lhcgr*$^{-/-}$ mice injected with PBS or AAV8-Lhcgr (n = 5). Arrows (A) and arrowheads (B) indicate the testes. Scale bar: 1 cm.

(C–J) Ano-genital distance (C), penile length (D), testis weight (E), epididymis weight (F), seminal vesicle weight (G), prostate weight (H), vas deferens weight (I), and vas deferens length (J) of *Lhcgr*$^{+/+}$ mice, *Lhcgr*$^{+/-}$ mice, and *Lhcgr*$^{-/-}$ mice injected with PBS or AAV8-Lhcgr (n = 5). Data are represented by boxplots, and whiskers show the minimum to maximum values. *p < 0.05; **p < 0.01; ***p < 0.001; ns, not significant.

In *Lhcgr*$^{-/-}$ mice treated with AAV8-Lhcgr (8×10^{10} gc/testis), the width of the seminiferous tubules was increased, and spermatogenesis was evident in these testes (Figure 3A). To further characterize spermatogenesis after gene therapy, epididymis samples were collected from the four groups 4 weeks after treatment. Histological analysis of the epididymis showed that the luminal diameters of tubules in the cauda were dramatically decreased in *Lhcgr*$^{-/-}$ mice compared with *Lhcgr*$^{+/+}$ or *Lhcgr*$^{+/-}$ group, and

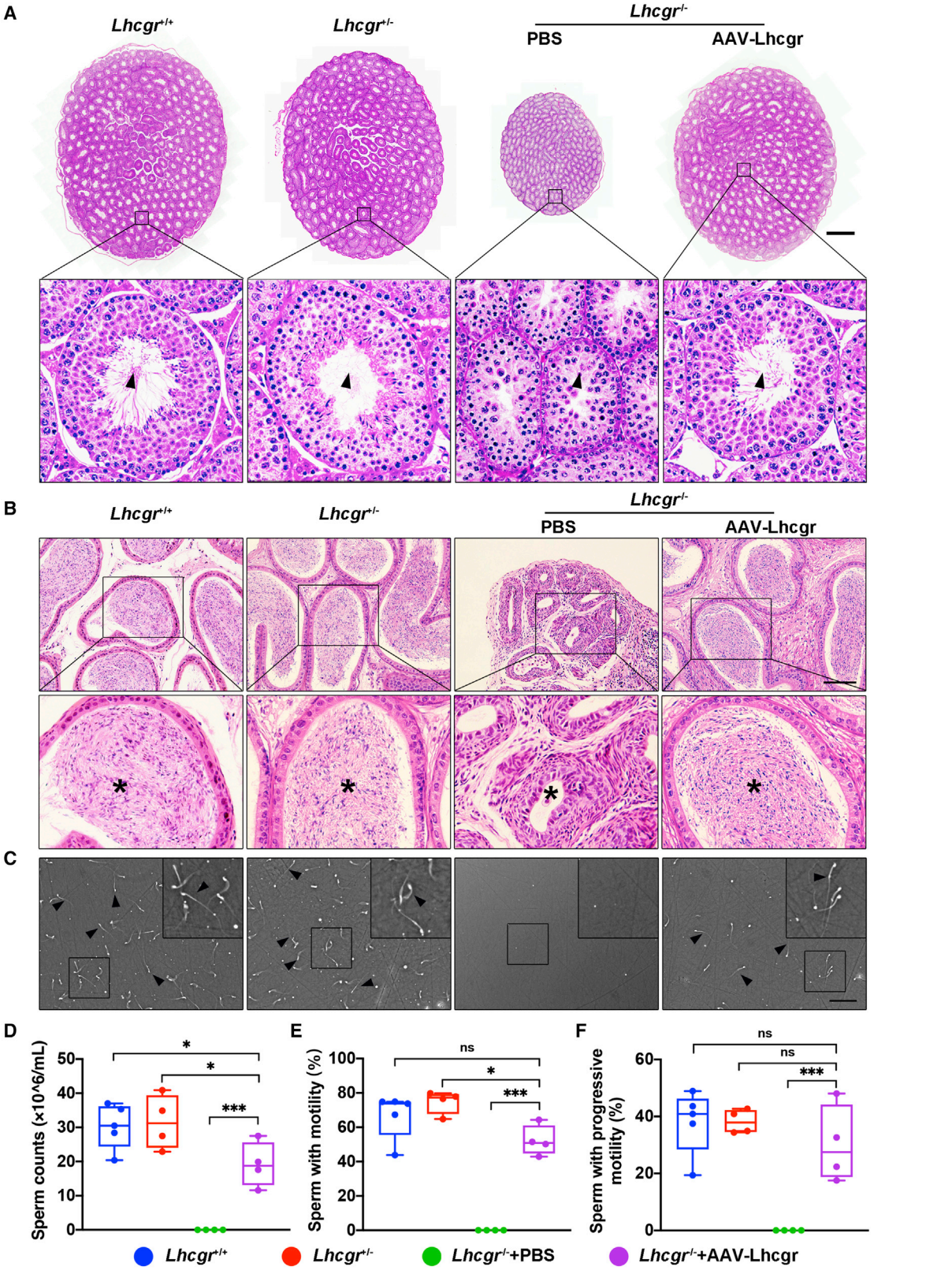

(legend on next page)

the lumens of the former were completely devoid of spermatozoa. Treatment of *Lhcgr*$^{-/-}$ mice with AAV8-Lhcgr (8 × 10^{10} gc/testis) restored the luminal diameter in the cauda epididymis and was associated with the presence of massive spermatozoa at this location (Figure 3B). To quantify the degree of spermatogenesis observed after AAV8-Lhcgr treatment, the quantity and motility of sperm were determined using a computer-aided semen analysis (CASA) system (Figure 3C). At 4 weeks post treatment, the epididymal sperm number of the AAV8-Lhcgr group was increased to over half of that observed in *Lhcgr*$^{+/+}$ and *Lhcgr*$^{+/-}$ mice, whereas sperm were not detected in PBS-treated *Lhcgr*$^{-/-}$ mice (Figure 3D). Analysis of sperm progressive motility revealed no apparent difference between the sperm of AAV8-Lhcgr-treated *Lhcgr*$^{-/-}$ mice and their *Lhcgr*$^{+/+}$ or *Lhcgr*$^{+/-}$ littermates (Figures 3E and 3F; Videos S1 and S2). Collectively, these results suggest that AAV8-Lhcgr rescues spermatogenesis and substantially increases sperm number and motility.

AAV8-Lhcgr promotes the formation of round and elongating spermatids

To molecularly define the consequences of AAV8-Lhcgr on spermatogenesis, RNA sequencing (RNA-seq) was performed 4 weeks after AAV8-Lhcgr (8 × 10^{10} gc/testis) treatment. RNA-seq analysis showed that AAV8-Lhcgr-injected testes of *Lhcgr*$^{-/-}$ mice had extremely high similarity in gene expression with *Lhcgr*$^{+/+}$ and *Lhcgr*$^{+/-}$ groups, whereas the PBS-treated *Lhcgr*$^{-/-}$ group showed less similarity with the other three groups (Figures S3A and S3B). Furthermore, we performed Gene Ontology (GO) analysis of the differentially expressed genes (DE-Gs) between PBS and AAV8-Lhcgr-treated *Lhcgr*$^{-/-}$ testes (Figure 4A). The results showed that upregulated genes were enriched for germ cell development and spermatid differentiation, indicating that processes involved in spermatogenesis were activated after AAV8-Lhcgr treatment. To determine the stages of spermatogenesis at which AAV8-Lhcgr gene therapy functions, we queried these data with functionally defined genes reflecting spermatogonia, spermatocytes, round spermatocytes, and elongating spermatids[24] and observed that the transcript profile of *Lhcgr*$^{-/-}$ testis treated with PBS was enriched for genes related to spermatogonia (e.g., *Dazl*, *Stra8*, and *Zbtb16*) and spermatocytes (e.g., *Tex101*, *Piwil1*, and *Sycp3*). However, AAV8-Lhcgr-treated samples were highly enriched in transcripts specific for round spermatids (e.g., *Acrv1*, *Tssk1*, *Spag6*, and *Spaca1*) and elongating spermatids (e.g., *Best1*, *Pabpc1*, *Ccdc89*, and *Prm1*) (Figure 4B). These results were further confirmed by quantitative RT-PCR analysis (Figures S3C–S3F). Immunofluorescence analysis of peanut agglutinin (PNA), which labels the acrosome, supported the appearance of spermatids in the testes of AAV8-Lhcgr-treated *Lhcgr*$^{-/-}$ mice, whereas PNA^{+} signals were extremely weak in the PBS-treated group (Figures 4C and 4D). Transition protein 2 (TNP2), which is expressed in the nuclei of elongating spermatids during the histone-to-protamine transition,[25] was barely detected in the testes of PBS-treated *Lhcgr*$^{-/-}$ mice, whereas its expression was clearly present in those of AAV8-Lhcgr-treated mice (Figures 4E and 4F). Together, these findings support the hypothesis that AAV8-Lhcgr treatment promotes the formation of round and elongating spermatids.

AAV8-Lhcgr restores fertility and produces fertile offspring

To assess whether the sperm produced after gene therapy could support reproduction, *in vitro* fertilization (IVF) was performed using spermatozoa obtained from the caudal epididymis of male *Lhcgr*$^{-/-}$ mice 4 weeks after AAV8-Lhcgr (8 × 10^{10} gc/testis) injection and oocytes harvested from female *Lhcgr*$^{+/+}$ mice (Figure 5A). Among a total of 723 eggs used for IVF, 178 (24.6%) successfully progressed to two-cell embryos *in vitro* (efficiency, 12.5%–42.4%). Of these two-cell embryos, 149 were transplanted into the uteri of eight pseudo-pregnant mice, which produced 58 offspring (efficiency, 9.6%–55.6%) (Figure 5B; Table S1). To confirm that the offspring were derived from the AAV8-Lhcgr-treated *Lhcgr*$^{-/-}$ male mice and *Lhcgr*$^{+/+}$ females, eight pups were subjected to PCR-based genotyping. The results showed that the eight pups carried the wild-type and mutated alleles at proportions consistent with Mendelian law (Figure 5C).

To test whether AAV8 was integrated into the genomes of the offspring, we performed PCR using vector-specific primers for the CAG promoter and the inserted *Lhcgr*. We analyzed the tail DNA of eight representative offspring born from the AAV8-Lhcgr transduction experiments but failed to detect any vector sequences (Figure 5D). We further carried out Southern blotting using tail DNA from the eight representative offspring and showed a lack of apparent signals in any of the offspring (Figure 5E). These findings indicate that AAV8 did not integrate into the genomes of offspring.

We next investigated whether the offspring created via AAV8-Lhcgr gene therapy could produce a second generation. Four mature males and four females generated from AAV8-Lhcgr-treated *Lhcgr*$^{-/-}$ mice were mated with corresponding *Lhcgr*$^{+/+}$ mice, and all were proven fertile by natural mating (Figures 5F, 5G, 5J, and 5K). Moreover, the offspring from AAV8-Lhcgr-treated *Lhcgr*$^{-/-}$ mice exhibited normal fertility compared with those of *Lhcgr*$^{+/-}$ mice (Figures 5H, 5I, 5L, and 5M).

Figure 3. AAV8-Lhcgr rescues spermatogenesis in pubertal *Lhcgr*$^{-/-}$ mice

(A) Representative light micrographs of testis sections from *Lhcgr*$^{+/+}$ mice, *Lhcgr*$^{+/-}$ mice, and *Lhcgr*$^{-/-}$ mice injected with PBS or AAV8-Lhcgr (n = 3). Scale bar: 500 μm. Arrowheads indicate full spermatogenesis in testes.

(B) Histological analysis of cauda epididymis collected from *Lhcgr*$^{+/+}$ mice, *Lhcgr*$^{+/-}$ mice, and *Lhcgr*$^{-/-}$ mice injected with PBS or AAV8-Lhcgr (n = 3). Stars indicate spermatozoa in the cauda epididymis. Scale bar: 100 μm.

(C) Representative light micrographs of sperm obtained from the cauda epididymis of *Lhcgr*$^{+/+}$ mice (n = 5), *Lhcgr*$^{+/-}$ mice (n = 4), and *Lhcgr*$^{-/-}$ mice injected with PBS (n = 4) or AAV8-Lhcgr (n = 4). Scale bar: 200 μm.

(D–F) The sperm counts (D), proportions of sperm with motility (E), and progressive motility (F) were analyzed (*Lhcgr*$^{+/+}$ mice [n = 5], *Lhcgr*$^{+/-}$ mice [n = 4], and *Lhcgr*$^{-/-}$ mice injected with PBS [n = 4] or AAV8-Lhcgr [n = 4]). Data are represented by boxplots, and whiskers show the minimum to maximum values. *p < 0.05; ***p < 0.001; ns, not significant.

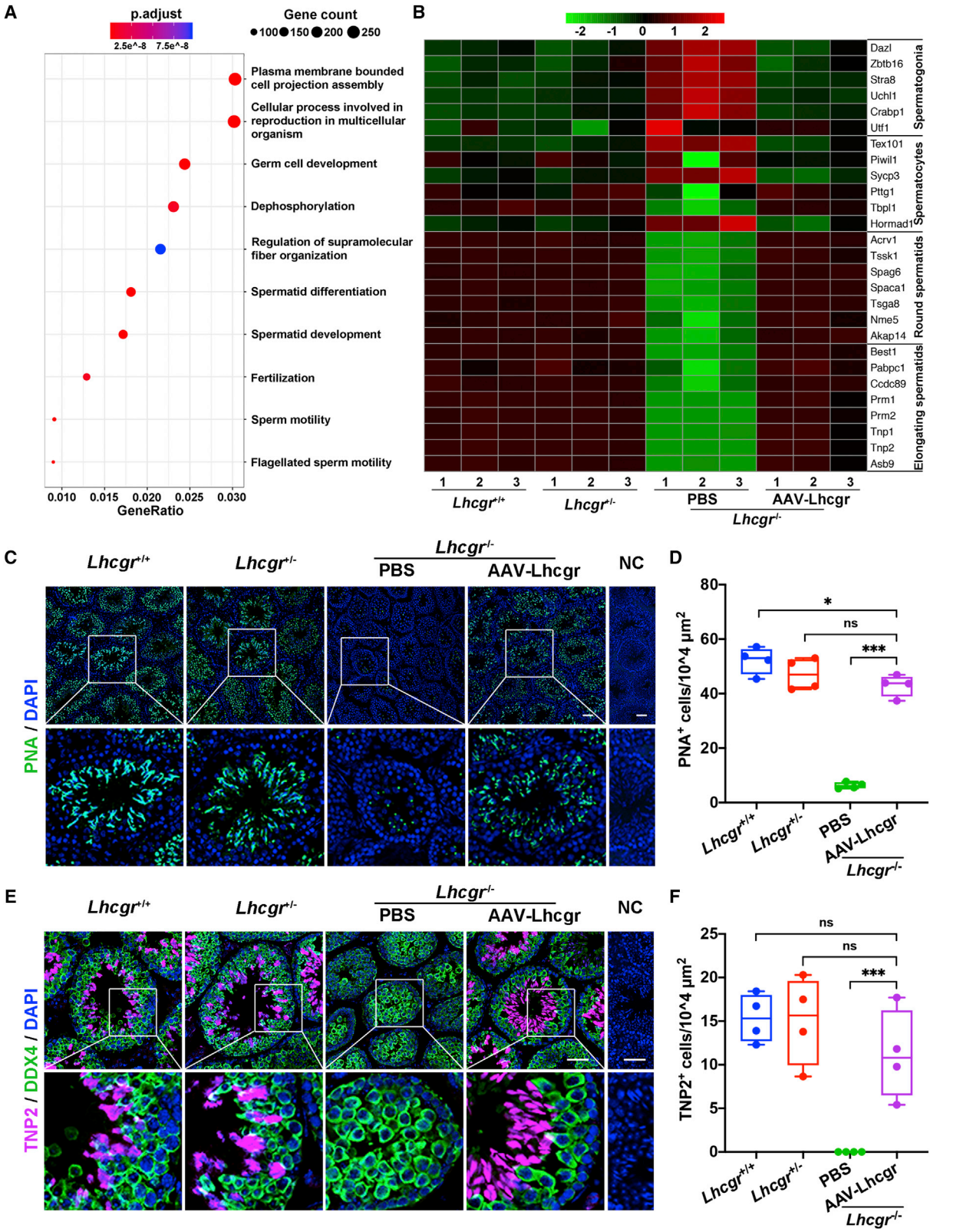

(legend on next page)

Collectively, AAV8-Lhcgr treatment in pubertal *Lhcgr*$^{-/-}$ mice gives rise to fertile offspring.

AAV-mediated gene therapy ensures long-term benefits with a single treatment

Next, we evaluated the long-term functional recovery of *Lhcgr*$^{-/-}$ mice 6 months after gene therapy (Figure 6A). Immunostaining demonstrated obvious LHCGR expression in the testicular interstitium in the AAV8-Lhcgr-treated group (8×10^{10} gc/testis), whereas LHCGR was negligibly detected in *Lhcgr*$^{-/-}$ mice treated with PBS (Figure 6B). Accordingly, serum and intratesticular testosterone concentrations were significantly increased in *Lhcgr*$^{-/-}$ mice treated with AAV8-Lhcgr compared with those receiving PBS (Figures 6C and 6D). Immunofluorescence analysis showed increased CYP17A1^{+} Leydig cell numbers in AAV-treated *Lhcgr*$^{-/-}$ mice compared with PBS-treated mice in the interstitial testicular space (Figure 6E). We also observed an obvious increase of masculinization in AAV-Lhcgr treated *Lhcgr*$^{-/-}$ mice compared with PBS-treated *Lhcgr*$^{-/-}$ mice (Figures 6F and 6G). Moreover, AAV8-Lhcgr-treated mice achieved significant recovery of spermatogenesis as determined by morphological changes of the testis (Figure 6H) and the presence of sperm in the caudal epididymis (Figure 6I). The recovery of spermatogenesis was also molecularly characterized by immunostaining for TNP2, which was greatly upregulated in AAV8-Lhcgr-treated *Lhcgr*$^{-/-}$ testes compared with PBS-treated testes (Figure 6J). At 6 months post treatment, we still observed significantly increased semen parameters in AAV8-Lhcgr-treated *Lhcgr*$^{-/-}$ mice, whereas sperm were not detected in PBS-treated *Lhcgr*$^{-/-}$ mice (Figures 6K–6M). Collectively, these results suggest that AAV8-Lhcgr ensures long-term benefits with a single treatment.

AAV8-Lhcgr recovers testosterone levels and rescues spermatogenesis in adult *Lhcgr*$^{-/-}$ mice

Because adult LCF patients miss the optimal opportunity for treatment at puberty,[26,27] we next questioned whether this approach still has therapeutic potential in adult mice. Eight-week-old *Lhcgr*$^{-/-}$ mice were injected with AAV8-Lhcgr (8×10^{10} gc/testis) and the effects were evaluated 4 weeks later (Figure 7A). Similar to the results obtained in the pubertal cohort, we found that administration of AAV8-Lhcgr to these adult *Lhcgr*$^{-/-}$ mice increased *Lhcgr* transcript expression and LHCGR protein levels in the testes compared with those in the PBS group (Figures 7B and S4A). Consistently, serum and intratesticular testosterone levels were recovered in AAV8-Lhcgr-injected *Lhcgr*$^{-/-}$ mice (Figures 7C and 7D). Serum dihydrotestosterone levels were also significantly increased in *Lhcgr*$^{-/-}$ mice treated with AAV8-Lhcgr compared with PBS in 8-week cohort at 4 weeks after treatment (Figure 7E). Immunofluorescence assays revealed the expression of the mature Leydig cell marker CYP17A1 (Figure S4B), suggesting that Leydig cell maturation occurred in AAV8-Lhcgr-treated *Lhcgr*$^{-/-}$ mice. We also observed normalization of sexual development in *Lhcgr*$^{-/-}$ mice after AAV8-Lhcgr treatment (Figures 7F, 7G, and S4C). Notably, AAV8-Lhcgr-treated mice achieved significant recovery of spermatogenesis as determined by morphological changes of the testis (Figure 7H), the presence of sperm in the caudal epididymis (data not shown), and significantly increased semen parameters (Figures 7I–7K). The recovery of spermatogenesis was also molecularly characterized by quantitative RT-PCR for round and elongating spermatid-specific genes and immunostaining for PNA and TNP2. These parameters were upregulated in AAV8-Lhcgr-treated *Lhcgr*$^{-/-}$ testes compared with PBS-treated testes (Figure S5).

To further investigate the time window of AAV8-Lhcgr gene therapy, 6-month-old mice were enrolled in the following experiments (Figure S6A). Consistent with our findings in the 3- and 8-week-old cohorts, we observed obvious expression of LHCGR (Figure S6B), improvements in testosterone levels (Figures S6C and S6D), maturation of Leydig cell (Figure S6E), and increase of masculinization in AAV8-Lhcgr-treated *Lhcgr*$^{-/-}$ mice (8×10^{10} gc/testis; Figures S6F and S6G). Moreover, AAV8-Lhcgr promoted spermatogenesis in these mice as inferred by the appearance of spermatids in testes and the existence of spermatozoa in the caudal epididymis from *Lhcgr*$^{-/-}$ mice treated with AAV8-Lhcgr (Figures S6H and S6I). Together, these data support the feasibility of using our AAV vector in mice that missed puberty and suggest that adulthood might not be an exclusion criterion for AAV-mediated gene therapy in potential LCF candidates.

Studies on non-human primate models form a translational bridge from small-animal models to humans. We further injected AAV8-mCherry particles into the testes of two pubertal male cynomolgus monkeys and performed histological analysis of the testes 7 days after vector injection. The results showed the co-expression of mCherry and the progenitor Leydig cell marker Nestin (Figure S7). In addition, immunofluorescence analysis revealed that mCherry was not co-expressed with the germ cell marker DDX4 or the Sertoli cell marker SOX9, indicating the absence of AAV infection in germ cells and Sertoli cells (Figure S7). Our results indicate that the interstitial injection of AAV8 could effectively target progenitor Leydig cells in pubertal male cynomolgus monkeys, reinforcing the feasibility and translational potential of AAV gene therapy in the testis.

DISCUSSION

We herein report the proof-of-concept study demonstrating that AAV-mediated gene therapy recovers testosterone production, restarts sexual development, rescues spermatogenesis, and restores fertility in the *Lhcgr*-deficient mouse model of LCF, suggesting that the AAV gene therapy strategy appears

Figure 4. AAV8-Lhcgr promotes the formation of elongating spermatids

(A) Representative GO terms of the top 500 upregulated genes in male *Lhcgr*$^{-/-}$ mice treated with AAV8-Lhcgr versus PBS (n = 3).

(B) Heatmap showing the expression of marker genes for the four major germ cell types in the testicular transcriptional profiles.

(C–F) Representative images of testis sections from the four groups (n = 4). Sections were immunostained for PNA (C), and DDX4 and TNP2 (E), and counterstained with DAPI. Quantitative analysis showing the percentage of PNA^{+} (D) and TNP2^{+} (F) germ cells in the seminiferous tubules of the testes. NC, negative control. Scale bar: 50 μm. Data are represented by boxplots, and whiskers show the minimum to maximum values. *p < 0.05; ***p < 0.001; ns, not significant.

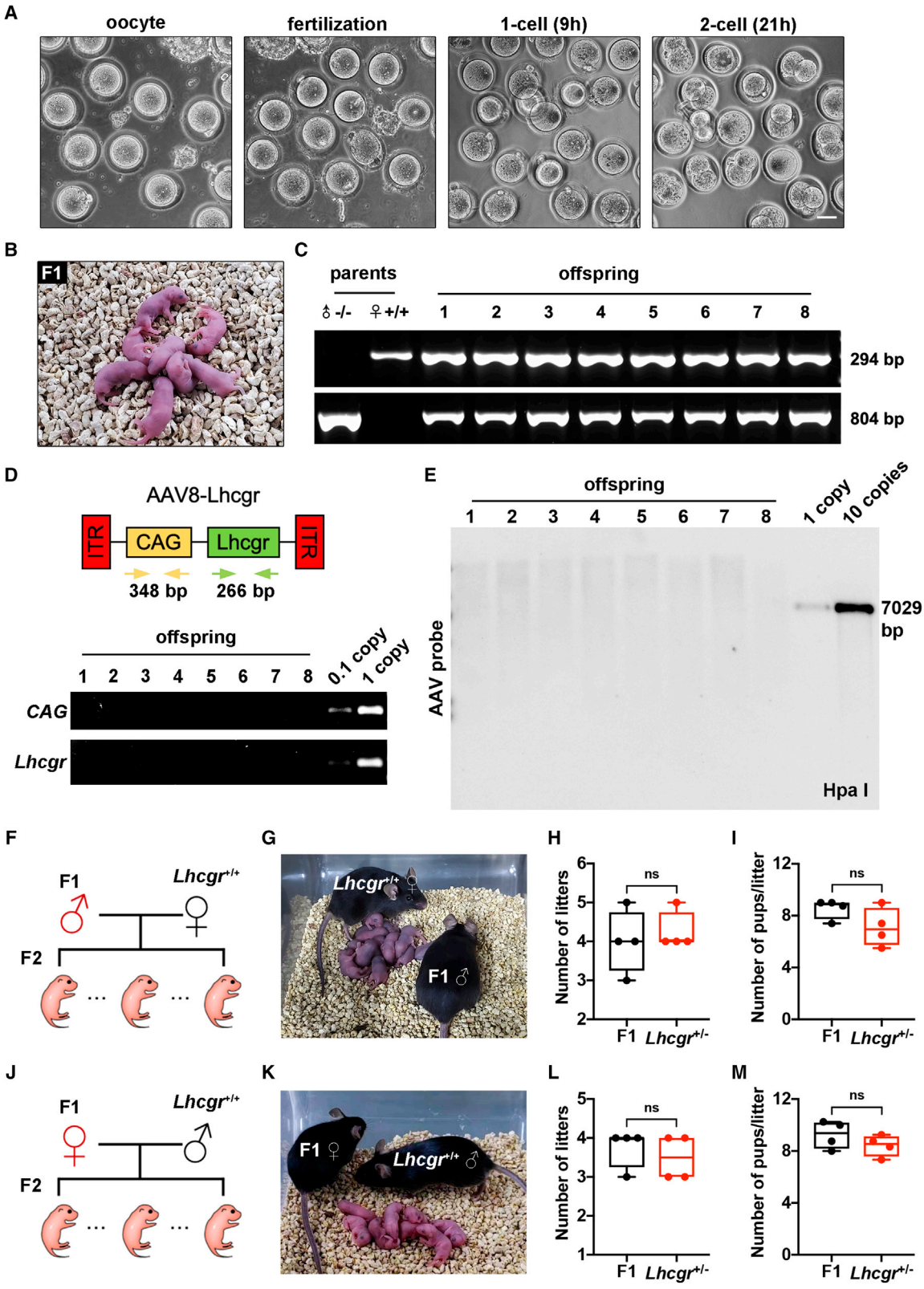

(legend on next page)

to be a promising treatment for LCF and thus may have value for future clinical applications.

Previous studies have shown that long-term TRT could recover serum testosterone levels and promote virilization in male pubertal *Lhcgr*$^{-/-}$ mice.[22,28] When the mean testosterone levels were approximately 4- to 8-fold higher than those in the wild-type group, TRT slightly stimulated the production of spermatozoa in the treated *Lhcgr*$^{-/-}$ mice.[22,28] However, exogenous testosterone beyond physical dosage can induce many serious adverse effects[29,30]; thus, it is not applicable in clinical practice. In this study, AAV8-mediated gene therapy in pubertal *Lhcgr*$^{-/-}$ mice partially increased serum testosterone levels and substantially improved sexual development. More importantly, modest testosterone restoration resulted in significant improvement in fertility. Testosterone restoration of approximately 30% in AAV8-Lhcgr-injected *Lhcgr*$^{-/-}$ mice recovered full spermatogenesis, produced fertilization-competent spermatozoa, and effectively gave rise to offspring. This might be due to the recovery of intratesticular testosterone and other nonsteroidal factors, which are vital for spermatogenesis.[6,31] Notably, these AAV8-Lhcgr gene therapy-derived mice restored fertility and produced the second generation by natural mating.

Ideally, gene therapy should be offered to patients at an early disease stage.[32] However, a large proportion of LCF patients are not diagnosed until adulthood.[26,27] To our surprise, we herein found that adult mice responded to AAV-mediated gene therapy as effectively as pubertal mice, as demonstrated by similar increments of testosterone production and restart of sexual development. Notably, we observed massive spermatozoa in the testis and caudal epididymis of *Lhcgr*$^{-/-}$ mice in adult cohorts after AAV8-Lhcgr treatment. Although IVF experiments were not conducted to evaluate the fertility of *Lhcgr*$^{-/-}$ mice treated at adult ages, we believe these sperm would generate zygotes and fertile offspring as observed in the pubertal cohort. This finding bodes well for translation into clinical application, meeting the urgent need of patients who have already reached adulthood at the time of diagnosis and who might be facing tremendous pressures related to fertility.[7]

There have been relatively few studies on gene transfer in the testis, possibly due to safety considerations.[10,33] By interstitially injecting into the testes of adult mice, Penny et al. found that adenoviral-mediated gene delivery is an expeditious way to probe Leydig cell function *in vivo*.[11] However, adenoviruses induced T lymphocyte infiltration in the testicular interstitium and its expression was gradually lost,[8,10,11] which limited the application of adenoviral-mediated gene targeting. In the present study, we have evaluated the safety of AAV8-mediated gene therapy from four aspects. First, AAV8 showed a clear tropism to target progenitor Leydig cells and showed an absence of infection in germ cells and Sertoli cells by interstitial injection in the testis of *Lhcgr*$^{-/-}$ mice; therefore, there was little chance of off-target transduction into other cells. Similarly, Satoshi and colleagues[10] did not observe infected germ cells or Sertoli cells following interstitial injection of AAV8. Second, we examined the infiltration of CD4^{+} and CD8^{+} T lymphocytes after AAV8 injection and there was no significant difference in lymphocyte infiltration between the two groups with or without injection, indicating that interstitial injection of AAV8 is safe and well tolerated. Third, we performed PCR and Southern blotting using tail DNA from the offspring born from AAV8-Lhcgr transduction experiments and did not detect any vector sequence signals in the offspring, suggesting that AAV8 did not integrate into the genomes of offspring. Fourth, given the importance of large animal models in translational research,[34] we also investigated the *in vivo* testes tissue tropism of AAV8 in non-human primate models. Consistent with the results of the mouse experiments, AAV8 targeted progenitor Leydig cells but not germ cells or Sertoli cells in monkey testes, reinforcing the safety and feasibility of AAV gene therapy in the testis. We recognize that the safety evaluation of gene therapy is critical and will pay attention to this issue.

AAV-mediated gene delivery is an accurate etiological treatment ideal for genetic diseases.[12] Based on the therapeutic effects of AAV8-Lhcgr on *Lhcgr*-deficient LCF mice, it is rational to hypothesize that AAV-mediated gene therapy exhibits strong potential to exert favorable effects on other types of genetic LCF, such as 3β-hydroxysteroid dehydrogenase type 2 (*3β-HSD2*) deficiency,[35] cytochrome P450 oxidoreductase (*POR*) deficiency,[36] *CYP17A1* deficiency,[37] or 17β-hydroxysteroid dehydrogenase type 3 (*17β-HSD3*) deficiency.[38] Although further studies are needed to thoroughly assess whether these types of LCF can be addressed by AAV8-mediated gene therapy, the present study sheds light on the ideal treatment of LCF, which

Figure 5. AAV8-Lhcgr restores fertility and produces fertile offspring

(A) Representative images of oocytes, fertilization, one-cell embryos, and two-cell embryos. Scale bar: 50 μm.

(B) Offspring (F1) derived from AAV8-Lhcgr-treated *Lhcgr*$^{-/-}$ male mice.

(C) Genotyping of the offspring derived from AAV8-Lhcgr-treated *Lhcgr*$^{-/-}$ males and *Lhcgr*$^{+/+}$ females. The amplified wild-type (wt) DNA is 294 bp, while the mutant (mt) DNA fragment is 804 bp.

(D) PCR analysis of AAV8-Lhcgr integration in the genomes of offspring. CAG promoter- and *Lhcgr*-specific primers were used. As a control, tail DNA from *Lhcgr*$^{+/-}$ mice was spiked with viral particles representing 0.1 and 1 copies of the viral genome.

(E) Southern blot analysis of DNA samples from offspring mice hybridized with AAV vector. Controls represent viral DNA in amounts equivalent to one and 10 copies of viral DNA per diploid genome. DNA was digested with the indicated restriction enzymes.

(F) Mating scheme used to produce the second-generation (F2) mice.

(G) Male F1 mice were used to produce F2 by mating with *Lhcgr*$^{+/+}$ females.

(H and I) Continuous breeding assay starting at 6 weeks of age, showing numbers of litters (H) and pups per litter (I) between F1 males and *Lhcgr*$^{+/-}$ males within 4 months (n = 4).

(J) Mating scheme used to produce F2 mice.

(K) Female F1 mice were used to produce F2 pups by mating with *Lhcgr*$^{+/+}$ males.

(L and M) Continuous breeding assay starting at 6 weeks of age, showing numbers of litters (L) and pups per litter (M) between F1 females and *Lhcgr*$^{+/-}$ females within 4 months (n = 4). Data are represented by boxplots, and whiskers show the minimum to maximum values. ns, not significant.

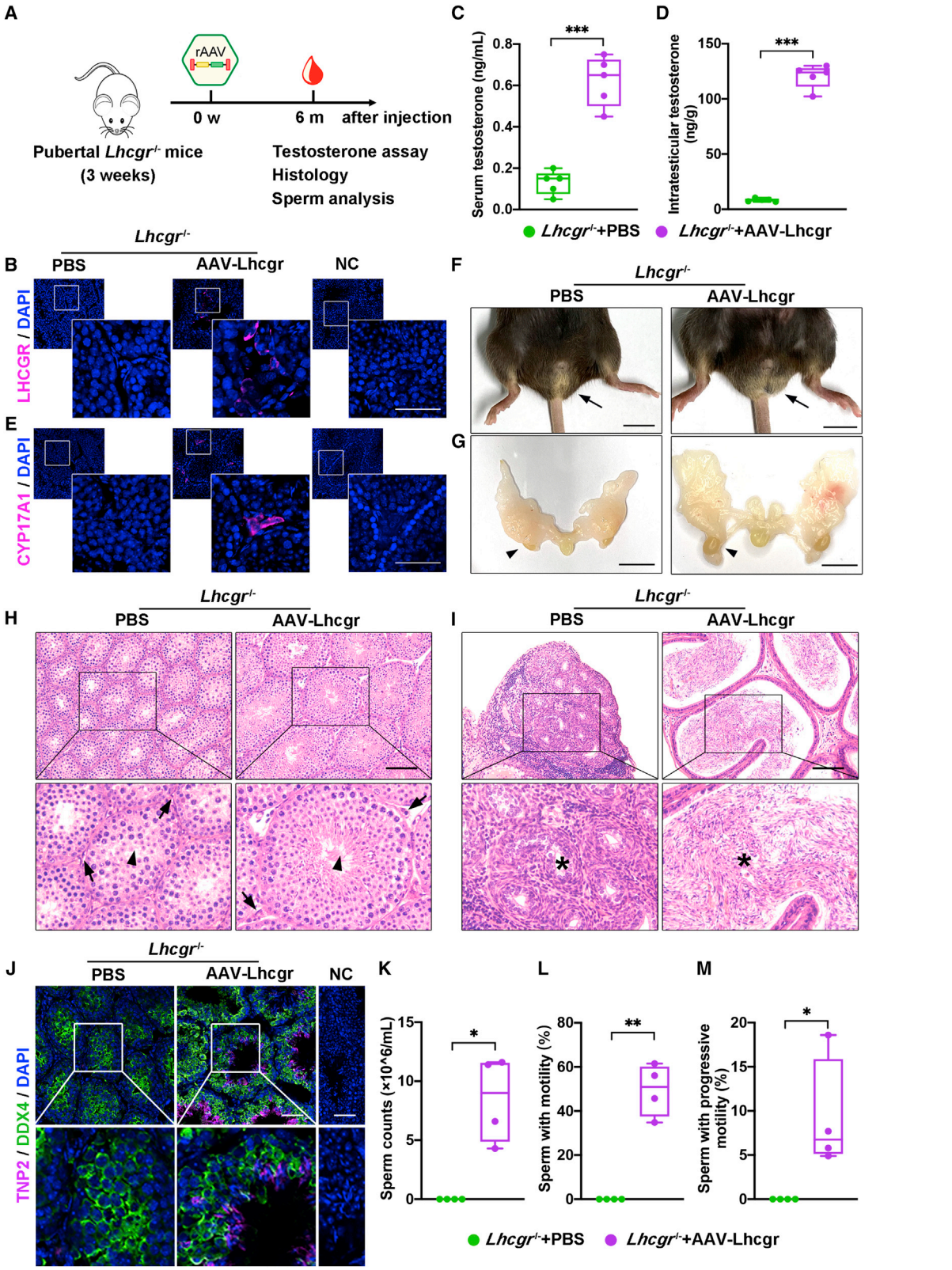

(legend on next page)

can potentially be expanded to more than 70 forms of genetic gonadal failure in an individualized manner.[39]

Limitations of the study

Progenitor Leydig cells have high proliferative capacities to expand the cell pool in order, eventually, to establish a right size of adult Leydig cells.[40,41] Although AAV8 targets up to 80% progenitor Leydig cells, the adult Leydig cell number and testosterone level were partially recovered. We speculate that the contradiction mainly results from the loss of the vector genome during progenitor Leydig cell proliferation because of the nonintegrating nature of AAV vectors. The present study indicates that gene therapy can restore spermatogenesis and produce fertile offspring; however, none of the gene-treated *Lhcgr*$^{-/-}$ mice sired offspring by natural mating for 3 months. The underlying reason is that partially recovered testosterone production is insufficient to support natural mating. Development of gene delivery tools that ensure more robust gene expression or correction of the pathogenic mutation by genome editing is worth trying to yield greater outcomes, including increased testosterone production and desirable recovery of fertility by natural mating.

STAR★METHODS

Detailed methods are provided in the online version of this paper and include the following:

SUPPLEMENTAL INFORMATION

Supplemental information can be found online at https://doi.org/10.1016/j.xcrm.2022.100792.

ACKNOWLEDGMENTS

The authors thank the Core Facilities of Medical Science for support in imaging experiments and are grateful to Yan Guo for her constructive suggestions, Rongda Deng for generously providing advice on testosterone detection, Zexin Guo for his assistance in semen analyses, and Yuan Qiu for her support of animal experiments.

Funding: This study was supported by the National Key Research and Development Program of China (2018YFA0107200, 2018YFA0801404); the Strategic Priority Research Program of the Chinese Academy of Sciences (XDA16020701); the National Natural Science Foundation of China (32130046, 81971314, 81901514, 82171564, 82101669, 81730005, 81721003); the Key Research and Development Program of Guangdong Province (2019B020235002); the Natural Science Foundation of Guangdong Province, China (2022A1515010371); and the Guangdong Special Support Plan (2019BT02Y276).

AUTHOR CONTRIBUTIONS

K.X. carried out the experiments, assisted with the experimental design, and wrote the manuscript. F.W. and L.D. carried out the experiments and data analysis. X.L. assisted with the design of the viral vector and assisted with the experimental design. P.L. and S.Z. performed animal experiments. H.C. assisted with IVF and data analysis. Y.M. and W.H. provided technical help in RNA-seq analysis. C.Y., W.O., Y.L., and X.F. assisted with animal experiments. B.Y. and C.L. helped with immunofluorescence staining. Z.L. provided *Lhcgr*$^{-/-}$ mice and assisted with manuscript revision. X.T., Q.K., and F.F.M. assisted with the experimental design and revised the manuscript. A.P.X. and C.D. conceived the project, supervised all experiments, and wrote and revised the manuscript. All authors fulfill the criteria for authorship.

DECLARATION OF INTERESTS

The authors declare no competing interests.

Figure 6. AAV-mediated gene therapy may ensure long-term benefits with a single treatment

(A) Experimental overview of the *in vivo* studies.

(B) Representative images of LHCGR expression in the testicular interstitium 6 months after treatment in *Lhcgr*$^{-/-}$ mice injected with PBS or AAV8-Lhcgr (n = 4). Nuclei were counterstained with DAPI. NC, negative control. Scale bar: 50 μm.

(C and D) The concentrations of serum (C) and intratesticular (D) testosterone were analyzed 6 months after treatment in 3-week-old *Lhcgr*$^{-/-}$ mice injected with PBS or AAV8-Lhcgr (n = 5).

(E) Representative images of CYP17A1expression in the testicular interstitium in *Lhcgr*$^{-/-}$ mice injected with PBS or AAV8-Lhcgr (n = 4). Nuclei were counterstained with DAPI. NC, negative control. Scale bar: 50 μm.

(F and G) Representative photographs of the external (F) and internal genitalia (G) of *Lhcgr*$^{-/-}$ mice injected with PBS or AAV8-Lhcgr (n = 4). Arrows (F) and arrowheads (G) indicate the testes. Scale bar: 1 cm.

(H and I) Representative light micrographs of testes (H) and epididymis (I) sections from *Lhcgr*$^{-/-}$ mice injected with PBS or AAV8-Lhcgr (n = 4). Arrows indicate Leydig cells, and arrowheads indicate full spermatogenesis in the testis (H). Stars indicate spermatozoa in the cauda epididymis (I). Scale bars: 100 μm.

(J) Representative images of testicular sections from *Lhcgr*$^{-/-}$ mice injected with PBS or AAV8-Lhcgr (n = 4). Sections were immunostained for DDX4 and TNP2 and counterstained with DAPI. Scale bars: 50 μm.

(K–M) The sperm counts (K) and proportions of sperm with motility (L) and progressive motility (M) were analyzed in *Lhcgr*$^{-/-}$ mice injected with PBS or AAV8-Lhcgr (n = 4). Data are represented by boxplots, and whiskers show the minimum to maximum values. *$p < 0.05$, **$p < 0.01$, ***$p < 0.001$.

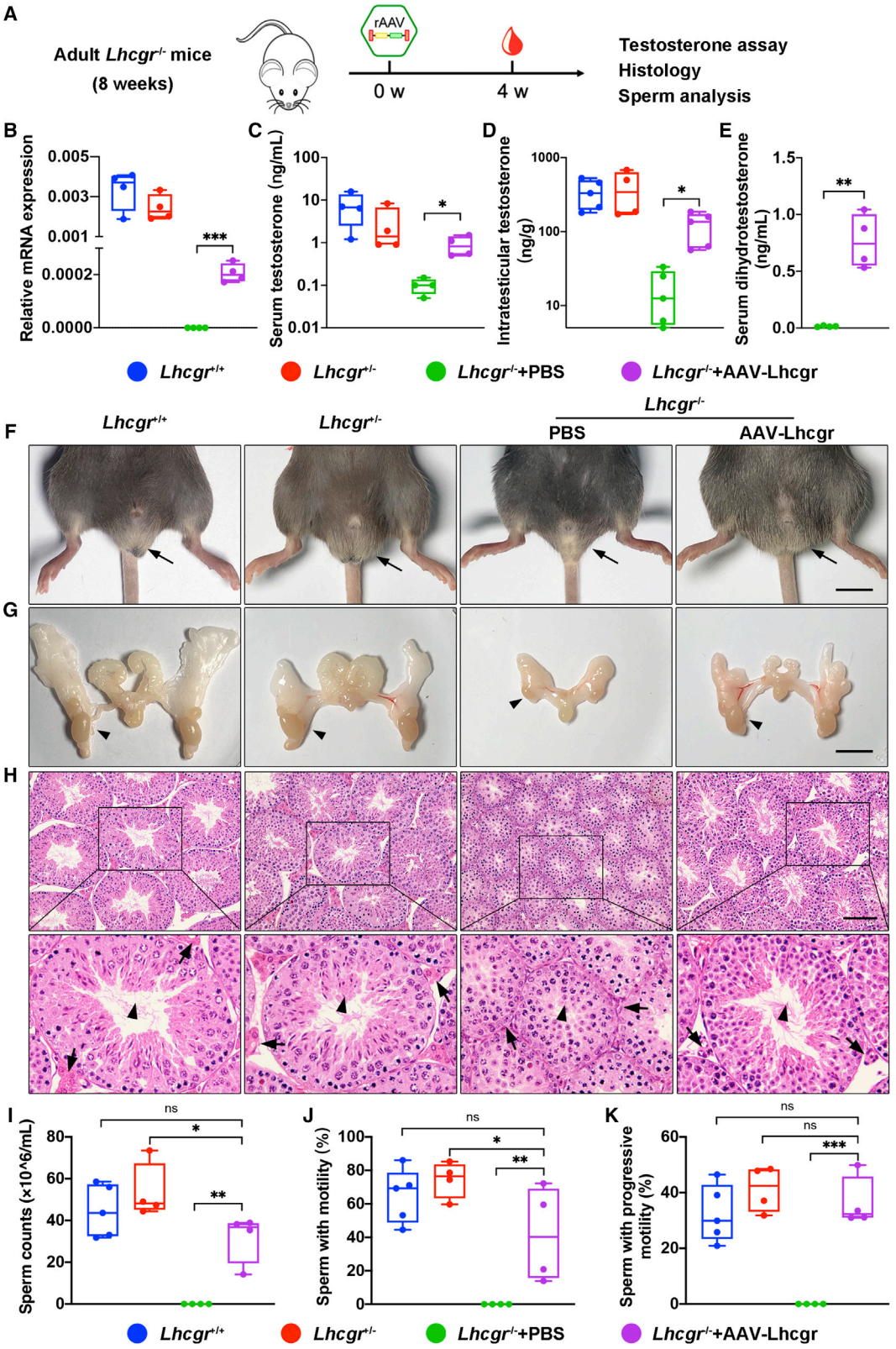

(legend on next page)

CellPress
OPEN ACCESS

Received: March 1, 2022
Revised: August 14, 2022
Accepted: September 28, 2022
Published: October 20, 2022

REFERENCES

1. Salonia, A., Rastrelli, G., Hackett, G., Seminara, S.B., Huhtaniemi, I.T., Rey, R.A., Hellstrom, W.J.G., Palmert, M.R., Corona, G., Dohle, G.R., et al. (2019). Paediatric and adult-onset male hypogonadism. Nat. Rev. Dis. Primers *5*, 38. https://doi.org/10.1038/s41572-019-0087-y.
2. Zirkin, B.R., and Papadopoulos, V. (2018). Leydig cells: formation, function, and regulation. Biol. Reprod. *99*, 101–111. https://doi.org/10.1093/biolre/ioy059.
3. Teerds, K.J., and Huhtaniemi, I.T. (2015). Morphological and functional maturation of Leydig cells: from rodent models to primates. Hum. Reprod. Update *21*, 310–328. https://doi.org/10.1093/humupd/dmv008.
4. Mendonca, B.B., Costa, E.M.F., Belgorosky, A., Rivarola, M.A., and Domenice, S. (2010). 46, XY DSD due to impaired androgen production. Best Pract. Res. Clin. Endocrinol. Metab. *24*, 243–262. https://doi.org/10.1016/j.beem.2009.11.003.
5. Bhasin, S., Brito, J.P., Cunningham, G.R., Hayes, F.J., Hodis, H.N., Matsumoto, A.M., Snyder, P.J., Swerdloff, R.S., Wu, F.C., and Yialamas, M.A. (2018). Testosterone therapy in men with hypogonadism: an endocrine society clinical practice guideline. J. Clin. Endocrinol. Metab. *103*, 1715–1744. https://doi.org/10.1210/jc.2018-00229.
6. Kathrins, M., and Niederberger, C. (2016). Diagnosis and treatment of infertility-related male hormonal dysfunction. Nat. Rev. Urol. *13*, 309–323. https://doi.org/10.1038/nrurol.2016.62.
7. Guercio, G., Costanzo, M., Grinspon, R.P., and Rey, R.A. (2015). Fertility issues in disorders of sex development. Endocrinol. Metab. Clin. North Am. *44*, 867–881. https://doi.org/10.1016/j.ecl.2015.07.012.
8. Darbey, A., Rebourcet, D., Curley, M., Kilcoyne, K., Jeffery, N., Reed, N., Milne, L., Roesl, C., Brown, P., and Smith, L.B. (2021). A comparison of in vivo viral targeting systems identifies adeno-associated virus serotype 9 (AAV9) as an effective vector for genetic manipulation of Leydig cells in adult mice. Andrology *9*, 460–473. https://doi.org/10.1111/andr.12915.
9. Yang, F., Whelan, E.C., Guan, X., Deng, B., Wang, S., Sun, J., Avarbock, M.R., Wu, X., and Brinster, R.L. (2021). FGF9 promotes mouse spermatogonial stem cell proliferation mediated by p38 MAPK signalling. Cell Prolif *54*, e12933. https://doi.org/10.1111/cpr.12933.
10. Watanabe, S., Kanatsu-Shinohara, M., Ogonuki, N., Matoba, S., Ogura, A., and Shinohara, T. (2018). In vivo genetic manipulation of spermatogonial stem cells and their microenvironment by adeno-associated viruses. Stem Cell Rep. *10*, 1551–1564. https://doi.org/10.1016/j.stemcr.2018.03.005.
11. Penny, G.M., Cochran, R.B., Pihlajoki, M., Kyrönlahti, A., Schrade, A., Häkkinen, M., Toppari, J., Heikinheimo, M., and Wilson, D.B. (2017). Probing GATA factor function in mouse Leydig cells via testicular injection of adenoviral vectors. Reproduction *154*, 455–467. https://doi.org/10.1530/REP-17-0311.
12. Wang, D., Tai, P.W.L., and Gao, G. (2019). Adeno-associated virus vector as a platform for gene therapy delivery. Nat. Rev. Drug Discov. *18*, 358–378. https://doi.org/10.1038/s41573-019-0012-9.
13. Pasi, K.J., Rangarajan, S., Mitchell, N., Lester, W., Symington, E., Madan, B., Laffan, M., Russell, C.B., Li, M., Pierce, G.F., and Wong, W.Y. (2020). Multiyear follow-up of AAV5-hFVIII-SQ gene therapy for hemophilia A. N. Engl. J. Med. *382*, 29–40. https://doi.org/10.1056/NEJMoa1908490.
14. Mendell, J.R., Sahenk, Z., Lehman, K., Nease, C., Lowes, L.P., Miller, N.F., Iammarino, M.A., Alfano, L.N., Nicholl, A., Al-Zaidy, S., et al. (2020). Assessment of systemic delivery of rAAVrh74.MHCK7.micro-dystrophin in children with duchenne muscular dystrophy: a nonrandomized controlled trial. JAMA Neurol. *77*, 1122–1131. https://doi.org/10.1001/jamaneurol.2020.1484.
15. Samaranch, L., Pérez-Cañamás, A., Soto-Huelin, B., Sudhakar, V., Jurado-Arjona, J., Hadaczek, P., Ávila, J., Bringas, J.R., Casas, J., Chen, H., et al. (2019). Adeno-associated viral vector serotype 9-based gene therapy for Niemann-Pick disease type A. Sci. Transl. Med. *11*, eaat3738. https://doi.org/10.1126/scitranslmed.aat3738.
16. Cehajic-Kapetanovic, J., Xue, K., Martinez-Fernandez de la Camara, C., Nanda, A., Davies, A., Wood, L.J., Salvetti, A.P., Fischer, M.D., Aylward, J.W., Barnard, A.R., et al. (2020). Initial results from a first-in-human gene therapy trial on X-linked retinitis pigmentosa caused by mutations in RPGR. Nat. Med. *26*, 354–359. https://doi.org/10.1038/s41591-020-0763-1.
17. Andres-Mateos, E., Landegger, L.D., Unzu, C., Phillips, J., Lin, B.M., Dewyer, N.A., Sanmiguel, J., Nicolaou, F., Valero, M.D., Bourdeu, K.I., et al. (2022). Choice of vector and surgical approach enables efficient cochlear gene transfer in nonhuman primate. Nat. Commun. *13*, 1359. https://doi.org/10.1038/s41467-022-28969-3.
18. Lei, Z.M., Mishra, S., Zou, W., Xu, B., Foltz, M., Li, X., and Rao, C.V. (2001). Targeted disruption of luteinizing hormone/human chorionic gonadotropin receptor gene. Mol. Endocrinol. *15*, 184–200. https://doi.org/10.1210/mend.15.1.0586.
19. Zhang, F.P., Pakarainen, T., Zhu, F., Poutanen, M., and Huhtaniemi, I. (2004). Molecular characterization of postnatal development of testicular steroidogenesis in luteinizing hormone receptor knockout mice. Endocrinology *145*, 1453–1463. https://doi.org/10.1210/en.2003-1049.
20. Rahman, N.A., and Rao, C.V. (2009). Recent progress in luteinizing hormone/human chorionic gonadotrophin hormone research. Mol. Hum. Reprod. *15*, 703–711. https://doi.org/10.1093/molehr/gap067.
21. Kossack, N., Troppmann, B., Richter-Unruh, A., Kleinau, G., and Gromoll, J. (2013). Aberrant transcription of the LHCGR gene caused by a mutation in exon 6A leads to Leydig cell hypoplasia type II. Mol. Cell. Endocrinol. *366*, 59–67. https://doi.org/10.1016/j.mce.2012.11.018.

Figure 7. AAV8-Lhcgr restarts sexual development and rescues spermatogenesis in adult *Lhcgr*-deficient mice

(A) Experimental overview of the *in vivo* studies.

(B) Quantitative RT-PCR was used to quantify *Lhcgr* mRNA transcripts in testis tissues from $Lhcgr^{+/+}$, $Lhcgr^{+/-}$, and $Lhcgr^{-/-}$ mice injected with PBS or AAV8-Lhcgr (n = 4). β-actin was used for normalization.

(C) The concentrations of serum testosterone were analyzed in $Lhcgr^{+/+}$, $Lhcgr^{+/-}$, and $Lhcgr^{-/-}$ mice injected with PBS or AAV8-Lhcgr (n = 4).

(D) The concentrations of intratesticular testosterone were analyzed in $Lhcgr^{+/+}$ (n = 5), $Lhcgr^{+/-}$ (n = 4), and $Lhcgr^{-/-}$ mice injected with PBS (n = 5) or AAV8-Lhcgr (n = 5).

(E) The concentrations of serum dihydrotestosterone testosterone were analyzed in $Lhcgr^{-/-}$ mice injected with PBS or AAV8-Lhcgr (n = 4).

(F and G) Representative photographs of the external and internal genitalia of mice from the four groups (n = 4). Arrows (F) and arrowheads (G) indicate the testes. Scale bar: 1 cm.

(H) Representative light micrographs of testis sections from four groups (n = 4). Arrows indicate Leydig cells and arrowheads indicate full spermatogenesis in the testis. Scale bars: 100 μm.

(I–K) The sperm counts (I), proportions of sperm with motility (J), and progressive motility (K) were analyzed ($Lhcgr^{+/+}$ [n = 5], $Lhcgr^{+/-}$ [n = 4], and $Lhcgr^{-/-}$ mice injected with PBS [n = 4] or AAV8-Lhcgr [n = 4]). Data are represented by boxplots, and whiskers show the minimum to maximum values. *$p < 0.05$; **$p < 0.01$; ***$p < 0.001$; ns, not significant.

22. Lei, Z.M., Mishra, S., Ponnuru, P., Li, X., Yang, Z.W., and Rao, C.V. (2004). Testicular phenotype in luteinizing hormone receptor knockout animals and the effect of testosterone replacement therapy. Biol. Reprod. *71*, 1605–1613. https://doi.org/10.1095/biolreprod.104.031161.

23. Welsh, M., Saunders, P.T.K., Fisken, M., Scott, H.M., Hutchison, G.R., Smith, L.B., and Sharpe, R.M. (2008). Identification in rats of a programming window for reproductive tract masculinization, disruption of which leads to hypospadias and cryptorchidism. J. Clin. Invest. *118*, 1479–1490. https://doi.org/10.1172/JCI34241.

24. Green, C.D., Ma, Q., Manske, G.L., Shami, A.N., Zheng, X., Marini, S., Moritz, L., Sultan, C., Gurczynski, S.J., Moore, B.B., et al. (2018). A comprehensive roadmap of murine spermatogenesis defined by single-cell RNA-seq. Dev. Cell *46*, 651–667.e10. https://doi.org/10.1016/j.devcel.2018.07.025.

25. Matzuk, M.M., McKeown, M.R., Filippakopoulos, P., Li, Q., Ma, L., Agno, J.E., Lemieux, M.E., Picaud, S., Yu, R.N., Qi, J., et al. (2012). Small-molecule inhibition of BRDT for male contraception. Cell *150*, 673–684. https://doi.org/10.1016/j.cell.2012.06.045.

26. Martens, J.W., Verhoef-Post, M., Abelin, N., Ezabella, M., Toledo, S.P., Brunner, H.G., and Themmen, A.P. (1998). A homozygous mutation in the luteinizing hormone receptor causes partial Leydig cell hypoplasia: correlation between receptor activity and phenotype. Mol. Endocrinol. *12*, 775–784. https://doi.org/10.1210/mend.12.6.0124.

27. Troppmann, B., Kleinau, G., Krause, G., and Gromoll, J. (2013). Structural and functional plasticity of the luteinizing hormone/choriogonadotrophin receptor. Hum. Reprod. Update *19*, 583–602. https://doi.org/10.1093/humupd/dmt023.

28. Pakarainen, T., Zhang, F.P., Mäkelä, S., Poutanen, M., and Huhtaniemi, I. (2005). Testosterone replacement therapy induces spermatogenesis and partially restores fertility in luteinizing hormone receptor knockout mice. Endocrinology *146*, 596–606. https://doi.org/10.1210/en.2004-0913.

29. Gagliano-Jucá, T., and Basaria, S. (2019). Testosterone replacement therapy and cardiovascular risk. Nat. Rev. Cardiol. *16*, 555–574. https://doi.org/10.1038/s41569-019-0211-4.

30. Tsametis, C.P., and Isidori, A.M. (2018). Testosterone replacement therapy: for whom, when and how? Metabolism *86*, 69–78. https://doi.org/10.1016/j.metabol.2018.03.007.

31. Sagata, D., Minagawa, I., Kohriki, H., Pitia, A.M., Uera, N., Katakura, Y., Sukigara, H., Terada, K., Shibata, M., Park, E.Y., et al. (2015). The insulin-like factor 3 (INSL3)-receptor (RXFP2) network functions as a germ cell survival/anti-apoptotic factor in boar testes. Endocrinology *156*, 1523–1539. https://doi.org/10.1210/en.2014-1473.

32. Manso, A.M., Hashem, S.I., Nelson, B.C., Gault, E., Soto-Hermida, A., Villarruel, E., Brambatti, M., Bogomolovas, J., Bushway, P.J., Chen, C., et al. (2020). Systemic AAV9.LAMP2B injection reverses metabolic and physiologic multiorgan dysfunction in a murine model of Danon disease. Sci. Transl. Med. *12*, eaax1744. https://doi.org/10.1126/scitranslmed.aax1744.

33. Rajasekaran, S., Thatte, J., Periasamy, J., Javali, A., Jayaram, M., Sen, D., Krishnagopal, A., Jayandharan, G.R., and Sambasivan, R. (2018). Infectivity of adeno-associated virus serotypes in mouse testis. BMC Biotechnol. *18*, 70. https://doi.org/10.1186/s12896-018-0479-1.

34. Knechtle, S.J., Shaw, J.M., Hering, B.J., Kraemer, K., and Madsen, J.C. (2019). Translational impact of NIH-funded nonhuman primate research in transplantation. Sci. Transl. Med. *11*, eaau0143. https://doi.org/10.1126/scitranslmed.aau0143.

35. Burckhardt, M.A., Udhane, S.S., Marti, N., Schnyder, I., Tapia, C., Nielsen, J.E., Mullis, P.E., Rajpert-De Meyts, E., and Flück, C.E. (2015). Human 3beta-hydroxysteroid dehydrogenase deficiency seems to affect fertility but may not harbor a tumor risk: lesson from an experiment of nature. Eur. J. Endocrinol. *173*, K1–K12. https://doi.org/10.1530/EJE-15-0599.

36. Miller, W.L. (2012). P450 oxidoreductase deficiency: a disorder of steroidogenesis with multiple clinical manifestations. Sci. Signal. *5*, pt11. https://doi.org/10.1126/scisignal.2003318.

37. Marsh, C.A., and Auchus, R.J. (2014). Fertility in patients with genetic deficiencies of cytochrome P450c17 (CYP17A1): combined 17-hydroxylase/17, 20-lyase deficiency and isolated 17, 20-lyase deficiency. Fertil. Steril. *101*, 317–322. https://doi.org/10.1016/j.fertnstert.2013.11.011.

38. Yang, Z., Ye, L., Wang, W., Zhao, Y., Wang, W., Jia, H., Dong, Z., Chen, Y., Wang, W., Ning, G., and Sun, S. (2017). 17beta-Hydroxysteroid dehydrogenase 3 deficiency: three case reports and a systematic review. J. Steroid Biochem. Mol. Biol. *174*, 141–145. https://doi.org/10.1016/j.jsbmb.2017.08.012.

39. Wisniewski, A.B., Batista, R.L., Costa, E.M.F., Finlayson, C., Sircili, M.H.P., Dénes, F.T., Domenice, S., and Mendonca, B.B. (2019). Management of 46, XY differences/disorders of sex development (DSD) throughout life. Endocr. Rev. *40*, 1547–1572. https://doi.org/10.1210/er.2019-00049.

40. Dombrowicz, D., Sente, B., Reiter, E., Closset, J., and Hennen, G. (1996). Pituitary control of proliferation and differentiation of Leydig cells and their putative precursors in immature hypophysectomized rat testis. J. Androl. *17*, 639–650.

41. Shiraishi, K., and Ascoli, M. (2007). Lutropin/choriogonadotropin stimulate the proliferation of primary cultures of rat Leydig cells through a pathway that involves activation of the extracellularly regulated kinase 1/2 cascade. Endocrinology *148*, 3214–3225. https://doi.org/10.1210/en.2007-0160.

42. Durinck, S., Spellman, P.T., Birney, E., and Huber, W. (2009). Mapping identifiers for the integration of genomic datasets with the R/Bioconductor package biomaRt. Nat. Protoc. *4*, 1184–1191. https://doi.org/10.1038/nprot.2009.97.

43. Wu, T., Hu, E., Xu, S., Chen, M., Guo, P., Dai, Z., Feng, T., Zhou, L., Tang, W., Zhan, L., et al. (2021). clusterProfiler 4.0: a universal enrichment tool for interpreting omics data. Innovation *2*, 100141. https://doi.org/10.1016/j.xinn.2021.100141.

44. Xia, K., Ma, Y., Feng, X., Deng, R., Ke, Q., Xiang, A.P., and Deng, C. (2020). Endosialin defines human stem Leydig cells with regenerative potential. Hum. Reprod. *35*, 2197–2212. https://doi.org/10.1093/humrep/deaa174.

45. Xia, K., Chen, H., Wang, J., Feng, X., Gao, Y., Wang, Y., Deng, R., Wu, C., Luo, P., Zhang, M., et al. (2020). Restorative functions of autologous stem Leydig cell transplantation in a testosterone-deficient non-human primate model. Theranostics *10*, 8705–8720. https://doi.org/10.7150/thno.46854.

46. Ernst, C., Eling, N., Martinez-Jimenez, C.P., Marioni, J.C., and Odom, D.T. (2019). Staged developmental mapping and X chromosome transcriptional dynamics during mouse spermatogenesis. Nat. Commun. *10*, 1251. https://doi.org/10.1038/s41467-019-09182-1.

47. Umehara, T., Tsujita, N., Zhu, Z., Ikedo, M., and Shimada, M. (2020). A simple sperm-sexing method that activates TLR7/8 on X sperm for the efficient production of sexed mouse or cattle embryos. Nat. Protoc. *15*, 2645–2667. https://doi.org/10.1038/s41596-020-0348-y.

STAR★METHODS

KEY RESOURCES TABLE

REAGENT or RESOURCE	SOURCE	IDENTIFIER
Antibodies		
Rabbit anti-PDGFRα	Abcam	Cat# ab203491; RRID: AB_2892065
Rabbit anti-Nestin	GeneTex	Cat# GTX133111; RRID: AB_2886832
Rabbit anti-DDX4	CST	Cat# 8761; RRID: AB_2797658
Rabbit anti-SOX9	Millipore	Cat# AB5535; RRID: AB_2239761
Rabbit anti-CYP17A1	CST	Cat# 94004; RRID: AB_2800219
Rabbit anti-α-SMA	Abcam	Cat# ab5694; RRID: AB_2223021
Rabbit anti-AIF1	GeneTex	Cat# GTX100042; RRID: AB_1240434
Mouse anti-LHCGR	Novus	Cat# NBP2-54479; RRID: NA
Mouse anti-TNP2	Santa Cruz	Cat# SC-393843; RRID: NA
Chicken anti-mCherry	Abcam	Cat# ab205402; RRID: AB_2722769
Rat Anti-Mouse CD4	BD	Cat# 557667; RRID: AB_396779
Rat Anti-Mouse CD8	BD	Cat# 557668; RRID: AB_396780
Goat Anti-rabbit Alexa Fluor 488	Invitrogen	Cat# A11037; RRID: AB_2534095
Goat Anti-rabbit Alexa Fluor 647	Invitrogen	Cat# A32733; RRID: AB_2633282
Goat Anti-mouse Alexa Fluor 647	Invitrogen	Cat# A32728; RRID: AB_2633277
Goat Anti-chicken Alexa Fluor 555	Invitrogen	Cat# A32932; RRID: AB_2762844
Bacterial and virus strains		
AAV-Lhcgr	Vigene Bioscience	N/A
AAV-mCherry	Vigene Bioscience	N/A
Chemicals, peptides, and recombinant proteins		
Avertin	Sigma-Aldrich	Cat# T48402
Triton X-100	Sigma-Aldrich	Cat# X100
Chorionic gonadotropin human (hCG)	Sigma-Aldrich	Cat# 1297001
Mineral oil	Sigma-Aldrich	Cat# M5310
Bouin's solution	Sigma-Aldrich	Cat# HT10132
DAPI	Invitrogen	Cat# P36966
PFA	Phygene	Cat# PH0427
Bovine Serum Albumin	Sigma-Aldrich	Cat# A7030
TYH Medium	This paper	N/A
KSOM Medium	This paper	N/A
Tissue-Tek® O.C.T. Compound	Sakura	Cat# 4583
Peanut agglutinin, PNA	Sigma	Cat# L7381; RRID: NA
Critical commercial assays		
RNeasy Kits	QIAGEN	Cat# 74116
Recombinant NovoScript 1st Strand cDNA Synthesis Kit	Novoprotein	Cat# E041
LightCycler® 480 SYBR Green I Master	Roche	Cat# 04887352001
TIANamp Genomic DNA kit	TIANGEN	Cat# 4992254
Deposited data		
Expression matrix	This paper	Database: https://ngdc.cncb.ac.cn/omix/ Project number: OMIX001301
Experimental models: Organisms/strains		
Mouse: Lhcgr+/− breeding pairs	Z.L. et al.[18]	N/A
Monkey: Cynomolgus monkey	Guangdong Blooming-spring Biological Technology Development Co., Ltd.	N/A

(*Continued on next page*)

Continued		
REAGENT or RESOURCE	SOURCE	IDENTIFIER
Oligonucleotides		
Primers used for quantitative RT-PCR, genotyping and integration assay	This Paper	Table S2
Software and algorithms		
SPSS 20.0	IBM	https://www.ibm.com/uk-en/analytics/spss-statistics-software
R v. 4.0.2		https://www.r-project.org
pheatmap v. 1.0.12	Raivo Kolde	https://cran.r-project.org/web/packages/pheatmap/index.html
biomaRt v. 2.46.3	Durinck Steffen et al.[42]	https://www.bioconductor.org/packages/release/bioc/html/biomaRt.html
clusterProfiler v. 4.0.5	T. Wu et al.[43]	https://www.bioconductor.org/packages/release/bioc/html/clusterProfiler.html
ggplot2 v. 3.3.5	Hadley Wickham et al.	https://cran.r-project.org/web/packages/ggplot2/index.html

RESOURCE AVAILABILITY

Lead contact

Further information and requests for resources and reagents should be directed to and will be fulfilled by the lead contact, Andy Peng Xiang (xiangp@mail.sysu.edu.cn).

Materials availability

All unique/stable reagents generated in this study are available from the lead contact with a completed Materials Transfer Agreement.

Data and code availability

The expression matrices presented in this study have been deposited in the OMIX repository (https://ngdc.cncb.ac.cn/omix/) with project number OMIX001301. This paper does not include the original code. Any additional information required to reanalyze the data in this paper is available from the lead contact upon request. All data associated with this study are presented in the paper or supplemental information.

EXPERIMENTAL MODEL AND SUBJECT DETAILS

Mice

A breeding colony was established from *Lhcgr* heterozygous (*Lhcgr*$^{+/-}$) C57BL/6 mice provided by Z.L.[18] Male mice were identified by PCR performed on DNA isolated from the tail as previously described[18] and were randomly assigned to experimental groups. All mice were maintained under controlled temperature (24 ± 1°C) and relative humidity (50–60%) with a standard 12-h light-and-dark cycle for the duration of the study.

Non-human primates

Two pubertal male cynomolgus monkeys (*Macaca fascicularis*; Blooming Spring Biological Technology Development Co., Ltd.) were used for the experiments. The monkeys were housed at the animal center of South China Agricultural University.

All animal experiments were carried out using protocols approved by the ICE for Clinical Research and Animal Trials of the First Affiliated Hospital of Sun Yat-sen University (No. 2020-003) and the Ethics Committee of South China Agricultural University (No. 2021-E001).

METHOD DETAILS

Experimental design

Male *Lhcgr*-deficient (*Lhcgr*$^{-/-}$) mice were injected interstitially with AAV vectors encoding Lhcgr at 3 weeks, 8 weeks, and 6 months of age. Sham-operated male littermates expressing wild-type *Lhcgr* (*Lhcgr*$^{+/+}$) or heterozygous for the null mutation (*Lhcgr*$^{+/-}$) were used as controls. The therapeutic readouts included testicular *Lhcgr* expression, testosterone levels, sexual development, histological evaluation, spermatogenesis assay, and fertility analyses. Experimental groups were sized to allow for statistical analysis and the sample size for each experiment is noted in the figure legends. Mice were assigned randomly to the experimental groups, and the

investigators responsible for assessing and measuring the results were blinded to the intervention. Strategies used for sample collection, treatment, and information processing are included in the results and STAR Methods sections.

Gene delivery in animal models

AAV viral vectors were prepared by Vigene Bioscience (Shandong, China). In brief, an AAV vector plasmid (pAAV-CAG-mCherry, pAAV-CAG-Lhcgr), an adenovirus helper plasmid (pHelper), and an AAV helper plasmid (pAAV-RC; pAAV1, pAAV2, pAAV6, pAAV8, and pAAV9) were transiently transfected into 293T cells. Recombinant AAV was harvested 72 h after transfection by three cycles of freezing and thawing. The crude viral lysate was then purified by fractionation with iodixanol-gradient centrifugation. Viral titers (in genome copies (gc)/mL) were determined by real-time PCR using Universal SYBR Green Mix (BIO-RAD, USA) and probes specific to the inverted terminal repeat sequence of the AAV vector. Vectors that passed quality control were aliquoted and stored at −80°C until use.

For interstitial injection of PBS or AAV vectors, we modified a previously reported method.[10] Briefly, mice were anesthetized with Avertin (250 mg/kg) by i.p. injection, the surgical site was sterilized with ethanol and a topical application of povidone-iodine. A single incision was made on the ventral skin and body wall approximately 1.5 cm anterior to the genitals, using sterile surgical scissors under aseptic conditions. The testes were pulled out by holding the fat pad. Care was taken not to injure the blood vessels. Each testis was immobilized by fine forceps, and AAV particles or PBS were injected into the testes using a 33-gauge needle syringe (Hamilton, Switzerland). The injection was performed into interstitial spaces (8 μL/testis) and the incision was sutured.

RNA extraction, cDNA synthesis, and quantitative RT-PCR

Total RNA was extracted from mouse testes using a RNeasy Kit (Qiagen, Germantown, MD, USA) according to the manufacturer's protocol. RNA purity was determined using a NanoDrop 1000 (Thermo Fisher Scientific, Wilmington, DE, USA). Reverse transcription was performed using a NovoScript® 1st Strand cDNA Synthesis Kit (Novoprotein, Shanghai, China). Quantitative RT-PCR was performed using LightCycler®480 SYBR Green I Master (Roche, Indianapolis, IN, USA), on a Light Cycler 480 Detection System (Roche). The primers used for quantitative RT-PCR are listed in Table S2. To validate the primers, a melting curve was generated to confirm a single peak and rule out the possibility of non-specific product or primer dimer formation. β-actin was amplified as a control, and the target gene expression levels were calculated using the ΔCt method and expressed relative to β-actin.

Immunofluorescence staining

Immunofluorescence staining was conducted as previously reported by our group.[44] The harvested testes were fixed with 4% PFA for 2 h at 4°C. The tissues were then dehydrated with 30% sucrose solution at 4°C for 24 h. Afterward, the tissues were soaked in Tissue-Tek O.C.T. Compound (Sakura Finetek, Torrance, CA, USA), frozen, and cryosectioned at 10 μm thickness using a frozen slicer (Leica CM1950). For intracellular protein detection, sections were permeabilized with 0.3% Triton X-100 (Sigma-Aldrich) for 30 min. The non-specific binding of antibodies was blocked with 3% BSA (Sigma-Aldrich) for 45 min at room temperature, and the slices were incubated overnight with primary antibodies at 4°C. The sections were then washed with PBS 3 times and incubated with secondary antibodies at room temperature for 45 min in the dark, and then for 5 min with DAPI. Finally, the specific fluorescence was visualized and photographed using an LSM800 confocal microscope (Zeiss, Jena, Germany) or a Leica DMi8 microscope (Leica, Wetzlar, Germany). The primary and secondary antibodies are listed in the key resources table.

Histological analysis

The testis and epididymis were collected, fixed overnight in Bouin's solution (Sigma-Aldrich), dehydrated in 75% ethanol, embedded in paraffin, and sectioned at 4 μm. The sections were deparaffinized with xylene, hydrated with graded ethanol, and stained with hematoxylin and eosin for histological analysis using an AxioScan.Z1 (Zeiss) or a Leica DMi8 microscope (Leica).

Sex hormone assays

Sex hormone concentrations were assayed as previously reported by our group.[45] Serum and testes samples were collected at the indicated time points and stored at −80°C until analysis. Testosterone levels were measured using a chemiluminescent immunoassay (CLIA) (KingMed Diagnostics Group Co., Ltd. Guangzhou, China). The coefficient of variation (CV) of CLIA is 2–5.1% for intra-assay precision and 2.6–5.2% for inter-assay precision. The minimum detectable dose of testosterone is 0.01 ng/mL.

Computer-aided semen analysis

Semen samples were analyzed as previously reported.[25] One cauda epididymis was removed from each mouse, incised with micro scissors, and incubated in 0.5 mL buffer containing 0.5% BSA (Sigma) for 15 min at 37°C to allow for sperm release. The tissue was removed, and sperm samples were diluted and analyzed using a Hamilton Thorne's Ceros II system. At least six fields were assessed for each sample, and the sperm concentration and percentages of motile and progressively motile spermatozoa were determined.

RNA-seq analysis

Total mRNA was isolated from the testes of *Lhcgr*$^{+/+}$ mice, *Lhcgr*$^{+/-}$ mice, and *Lhcgr*$^{-/-}$ mice injected with PBS or AAV8-Lhcgr. RNA sequencing libraries were constructed using an Illumina mRNA-seq Prep Kit (Illumina, San Diego, CA, USA) as recommended by the manufacturer. The fragmented and randomly primed 150-bp paired-end libraries were sequenced using an Illumina HiSeq X Ten. The

sequencing data were processed using Consensus Assessment of Sequence and Variation (CASAVA, version 1.8.2; Illumina) with the default settings. The transcripts per million (TPM) values were used to evaluate the expression levels of genes. Pearson correlation coefficient (PCC) values and heatmaps of the global gene expression profiles were generated to measure the similarities of the different samples. Differentially expressed genes (DE-Gs) between PBS-treated and AAV-Lhcgr-treated *Lhcgr*$^{-/-}$ testes were analyzed, and the relevant biological processes were identified by Gene Ontology (GO) analysis. Finally, the RNA-Seq data were analyzed in R version 4.0.2 to categorize the defined genes that characterized spermatogonia, spermatocytes, round spermatocytes, and elongating spermatids.[24,46]

In vitro fertilization (IVF) and mouse embryo transfer

IVF was conducted as previously described.[47] Sperm were collected from the cauda epididymis of *Lhcgr*$^{-/-}$ mice (7 weeks old) at 4 weeks after AAV8-Lhcgr injection, and then incubated in a humidified atmosphere of 5% CO2 in air at 37°C for 2 h in a 200 μL drop of TYH medium covered with mineral oil (Sigma-Aldrich) for sperm capacitation. Cumulus-oocyte complexes were collected from the oviducts of wild-type female C57BL/6 mice at 16 h after ovulatory hCG (Sigma-Aldrich) injection and placed in a 50 μL drop of TYH medium that was then covered with mineral oil (Sigma-Aldrich). IVF was performed by adding *in vitro*-capacitated sperm (approximately 10,000 sperm/50 μL) into the medium containing the oocytes. After 4 h, the oocytes were collected and transferred to the developing medium, KSOM. All zygotes were then washed and transferred into KSOM medium, and cultured in a humidified atmosphere of 5% CO2 in air at 37°C. The numbers of 2-cell embryos were determined at 21 h after insemination. The two-cell embryo formation rate was calculated by dividing the number of 2-cell embryos by the number of zygotes examined. For embryo transfer, we mated 8- to 12-week-old females with vasectomized males and determined whether they were pseudo-pregnant by monitoring the presence of a vaginal plug. Two-cell embryos were surgically transferred into the uterine horn of each pseudo-pregnant female.

Analysis of AAV8-Lhcgr integration in the offspring

To test whether AAV8 integrated into the genome of offspring, we applied a previously reported method.[10] Total DNA was extracted from the tail using a TIANamp Genomic DNA kit (TIANGEN, Beijing, China) according to the manufacturer's instructions. Genome integrations were quantified by PCR using specific primers for the CAG promoter and the inserted *Lhcgr*. PCR was performed using a Bio-Rad T100 following the manufacturer's protocol. The primers used for PCR are listed in Table S2. To detect viral DNA by Southern blotting, we digested 10 μg of DNA from offspring and AAV-Lhcgr plasmid with the indicated restriction enzymes and separated the fragments by electrophoresis on a 0.7% agarose gel. DNA was transferred and blotted onto a Hybond N+ nylon membrane (Amersham Biosciences, UK). The probe targeting AAV was synthesized and labeled with digoxigenin-dUTP (PCR DIG Probe Synthesis Kit, Roche). Hybridization was performed by Zoonbio Biotechnology Co., Ltd (Nanjing, China) using a DIG DNA labeling and detection kit (Roche). The hybridized membrane was detected in the presence of CSPD (C18H20ClNa2O7P), and the hybridized signals were visualized on X-ray film. The primers used for probe synthesis are listed in Table S2.

QUANTIFICATION AND STATISTICAL ANALYSIS

All data were analyzed using SPSS 20.0 software (IBM SPSS Statistics, Armonk, NY, USA). Statistical differences between samples were assessed with Student's t-tests, one-way analysis of variance (ANOVA), or nonparametric tests (Mann-Whitney U tests and Kruskal-Wallis test). Differences were considered significant when $p < 0.05$ (*$p < 0.05$, **$p < 0.01$ and ***$p < 0.001$), ns = not significant.

Cell Reports Medicine, Volume *3*

Supplemental information

AAV-mediated gene therapy produces fertile offspring in the *Lhcgr*-deficient mouse model of Leydig cell failure

Kai Xia, Fulin Wang, Xingqiang Lai, Lin Dong, Peng Luo, Suyuan Zhang, Cuifeng Yang, Hong Chen, Yuanchen Ma, Weijun Huang, Wangsheng Ou, Yuyan Li, Xin Feng, Bin Yang, Congyuan Liu, Zhenmin Lei, Xiang'an Tu, Qiong Ke, Frank Fuxiang Mao, Chunhua Deng, and Andy Peng Xiang

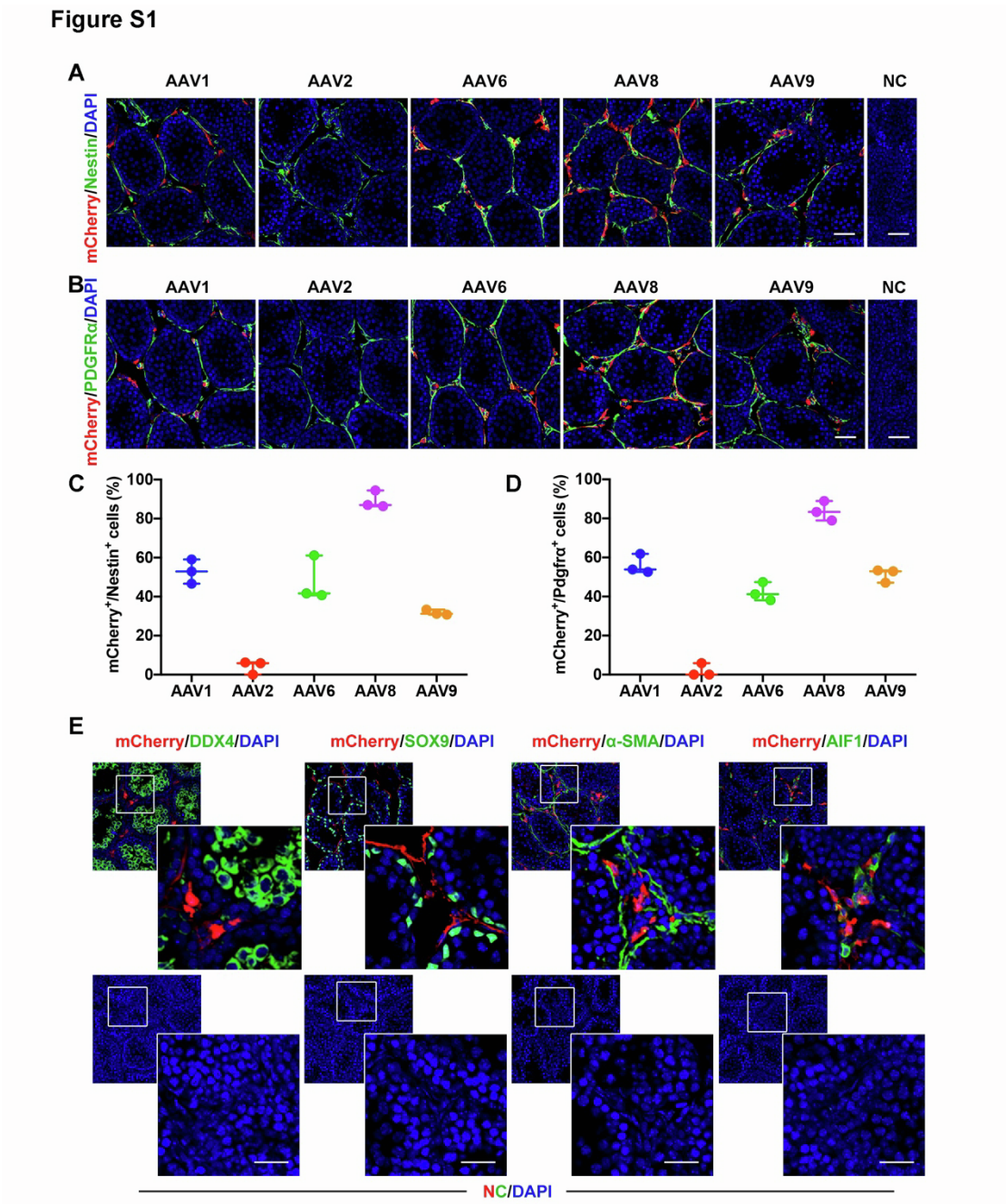

Figure S1. Testicularly injected AAV8 targets progenitor Leydig cells. Related to Figure 1.
(A and B) Representative confocal images of the testicular sections of *Lhcgr*$^{-/-}$ mice injected with AAV-CAG-mCherry (n=3) of the indicated capsid serotypes. The testis tissues were collected and immunostained with progenitor Leydig cells markers (Nestin, PDGFRα) at 7 days after AAV injection. NC indicates negative control. Scale bars: 50 μm. (C and D) Viral transduction rates were determined from the number of mCherry^{+} cells divided by the number of Nestin^{+} or PDGFRα^{+} progenitor Leydig cells. Data are represented by plots, and whiskers are minimum to maximum values. (E) Immunostaining of AAV8-mCherry-injected testes for the germ cell marker DDX4, or the Sertoli cell marker SOX9, peritubular myoid cells marker α-SMA, and macrophage markers AIF1 at 7 days after injection. Nuclei were counterstained with DAPI. NC indicates negative control. Scale bar: 25 μm.

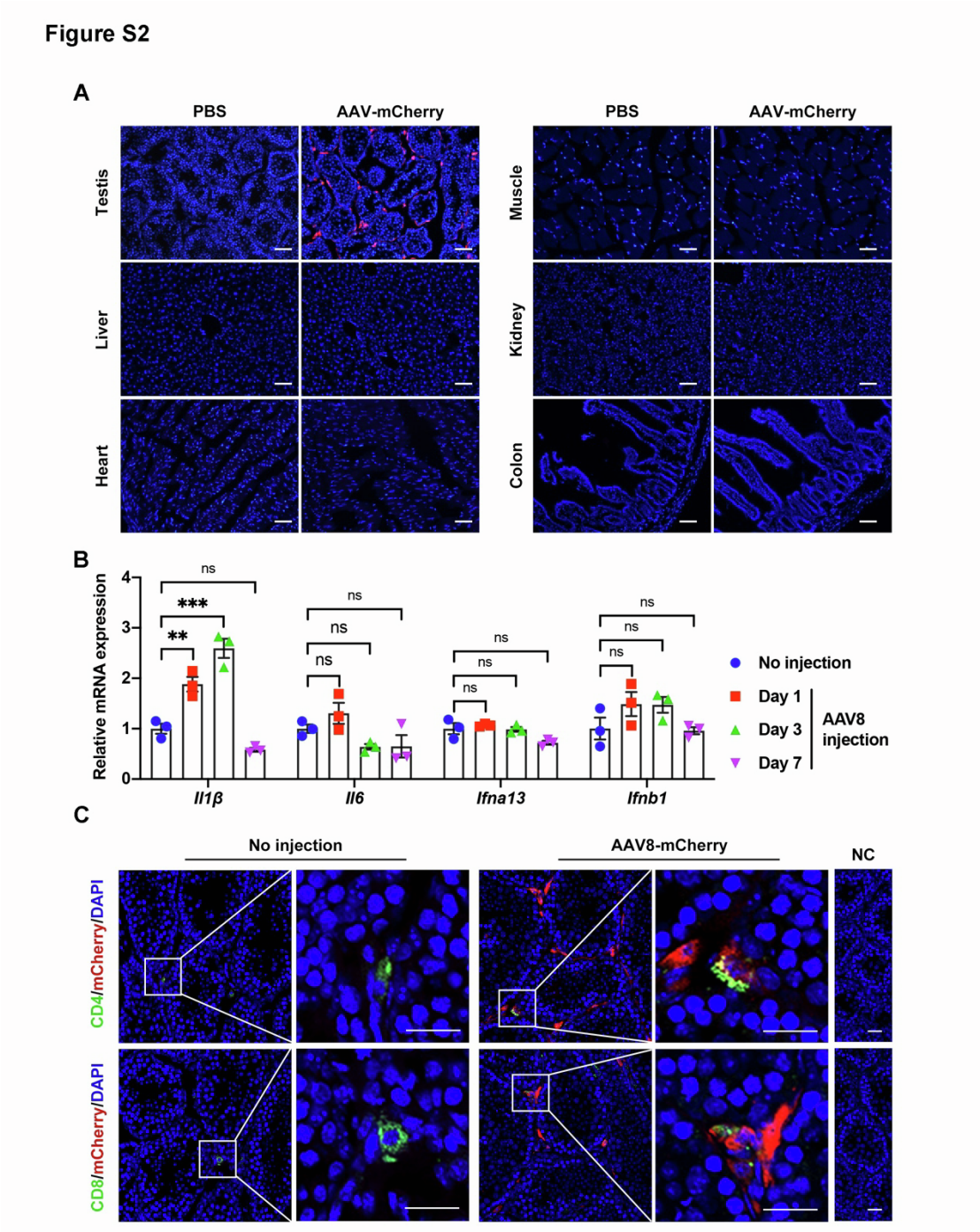

Figure S2. AAV8 showed a clear testis tropism and safety profile with no apparent inflammatory reaction. Related to Figure 1.

(A) Representative fluorescent photographs of mCherry expression (red) in indicated organs of AAV8-mCherry treated mice for 4 weeks. Scale bar: 50 μm. (B) Quantitative RT-PCR was used to analyze key inflammatory markers expression in testes samples collected from *Lhcgr*$^{-/-}$ mice on days 1, 3, and 7 following AAV-mCherry injection, respectively. β-actin was used for normalization. Data are expressed as mean ± sem. * $p < 0.05$, ** $p < 0.01$, *** $p < 0.001$, ns = not significant. (C) Immunostaining of *Lhcgr*$^{-/-}$ mouse testes by CD4 and CD8 antibodies 7 days after microinjection AAV8-mCherry into the interstitium. NC indicates negative control. Scale bar: 50 μm.

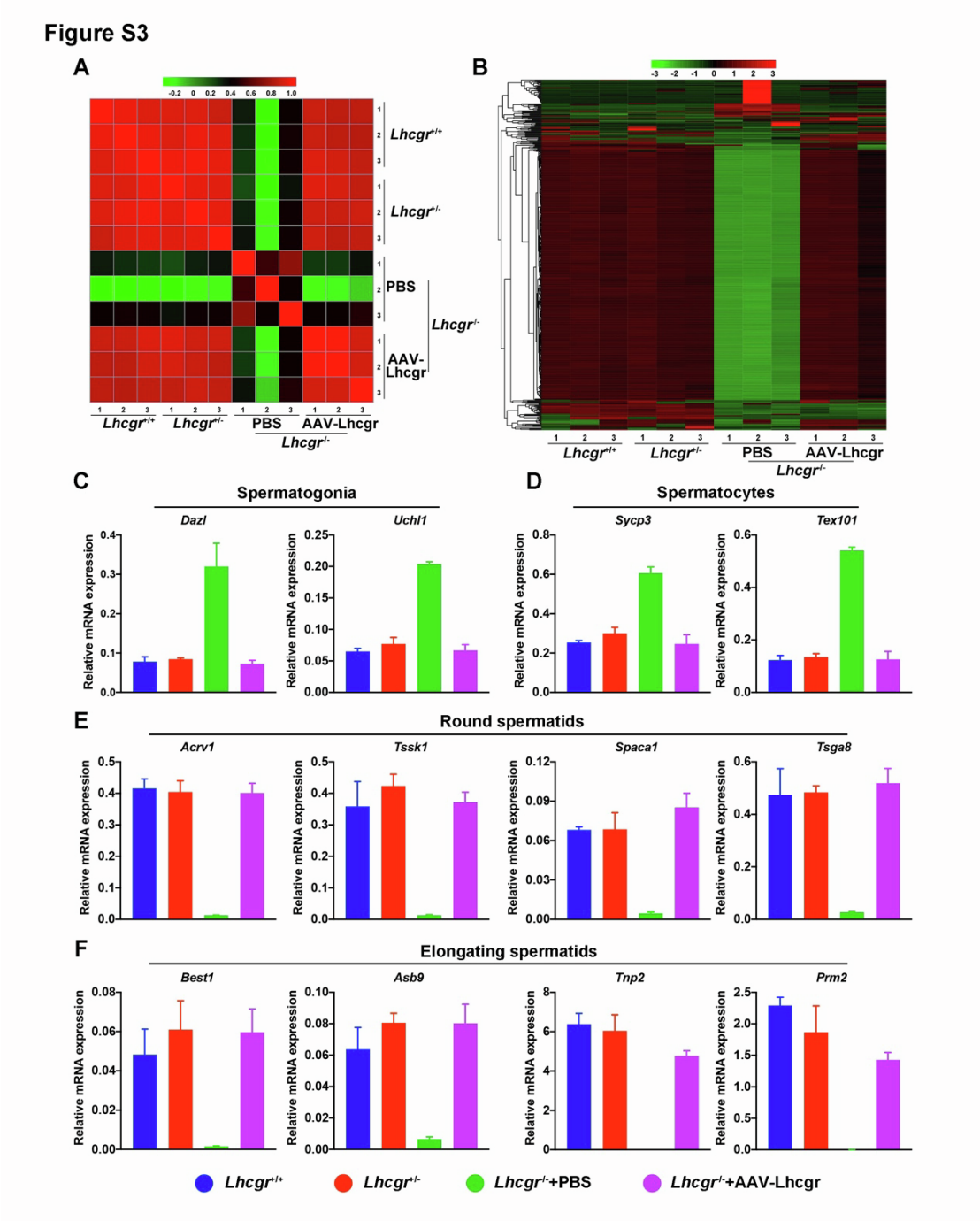

Figure S3. Testicular transcriptome profiles and mRNA expression of specific germ cell marker genes 4 weeks after treatment in pubertal cohort. Related to Figure 4.

(A) Pearson correlation coefficient (PCC) values were calculated to identify the correlation among *Lhcgr*$^{+/+}$ mice, *Lhcgr*$^{+/-}$ mice, and *Lhcgr*$^{-/-}$ mice injected with PBS or AAV8-Lhcgr (n=3). Each symbol represents an individual sample. (B) Heat map of top 500 gene expression profiles in the testes of *Lhcgr*$^{+/+}$ mice, *Lhcgr*$^{+/-}$ mice, and *Lhcgr*$^{-/-}$ mice injected with PBS or AAV8-Lhcgr (n=3). The color code indicates z-score-normalized expression values. (C-F) Quantitative RT-PCR analysis was performed in testes samples collected from *Lhcgr*$^{+/+}$ mice, *Lhcgr*$^{+/-}$ mice, and *Lhcgr*$^{-/-}$ mice injected with PBS or AAV8-Lhcgr (n=3) at 4 weeks after treatment. The expression levels of marker genes for spermatogonia (*Dazl*, *Uchl1*), spermatocytes (*Sycp3*, *Tex101*), round spermatids (*Acrv1*, *Tssk1*, *Spaca1*,

and *Tsga8*), and elongating spermatids (*Best1*, *Asb9*, *Tnp2*, and *Prm2*) were detected from each group. Data are expressed as mean ± sem.

Figure S4

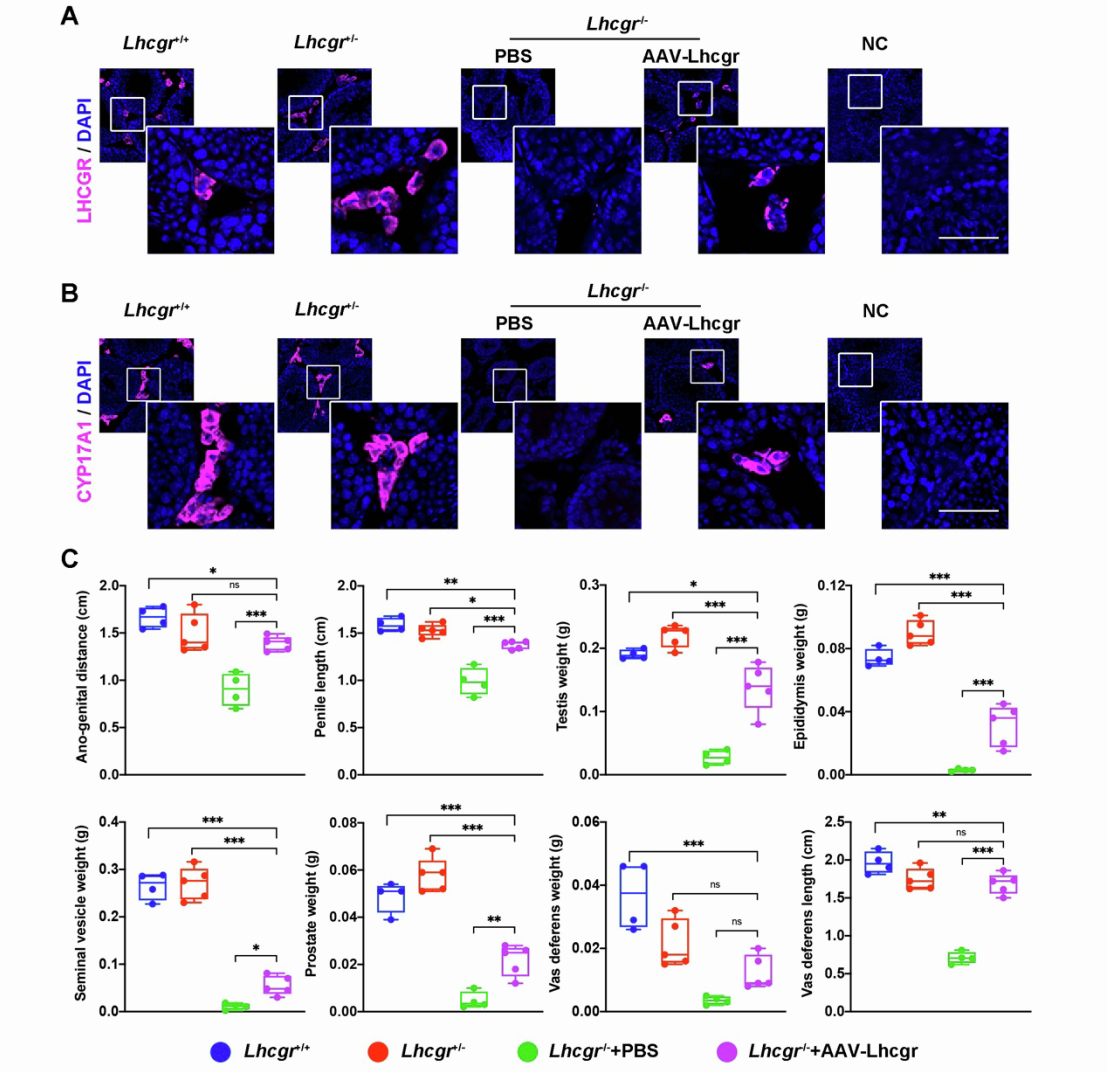

Figure S4. Testicular injection of AAV8-Lhcgr rescues Leydig cell function and restarts sexual development in 8-week-old adult *Lhcgr*$^{-/-}$ mice. Related to Figure 7.

(A) Representative images of LHCGR expression in the testicular interstitium at 4 weeks after treatment in 8 weeks *Lhcgr*$^{+/+}$ mice, *Lhcgr*$^{+/-}$ mice, and *Lhcgr*$^{-/-}$ mice injected with PBS or AAV8-Lhcgr (n=4). Nuclei were counterstained with DAPI. NC indicates negative control. Scale bar: 50 μm. (B) The Leydig cells marker, CYP17A1, was evaluated in the testicular interstitium by immunofluorescence assay at 4 weeks after treatment in *Lhcgr*$^{+/+}$ mice, *Lhcgr*$^{+/-}$ mice, and *Lhcgr*$^{-/-}$ mice injected with PBS or AAV8-Lhcgr (n=4). NC indicates negative control. Scale bar: 50 μm. (C) The ano-genital distance, penile length, testis weight, epididymis weight, seminal vesicle weight, prostate weight, vas deferens weight, and vas deferens length of *Lhcgr*$^{+/+}$ mice (n=4), *Lhcgr*$^{+/-}$ mice (n=5), *Lhcgr*$^{-/-}$ mice injected with PBS (n=4) or AAV8-Lhcgr (n=5) at 4 weeks after treatment. Data are represented by box plots, and whiskers are minimum to maximum values. * $p < 0.05$, ** $p < 0.01$, *** $p < 0.001$, ns = not significant.

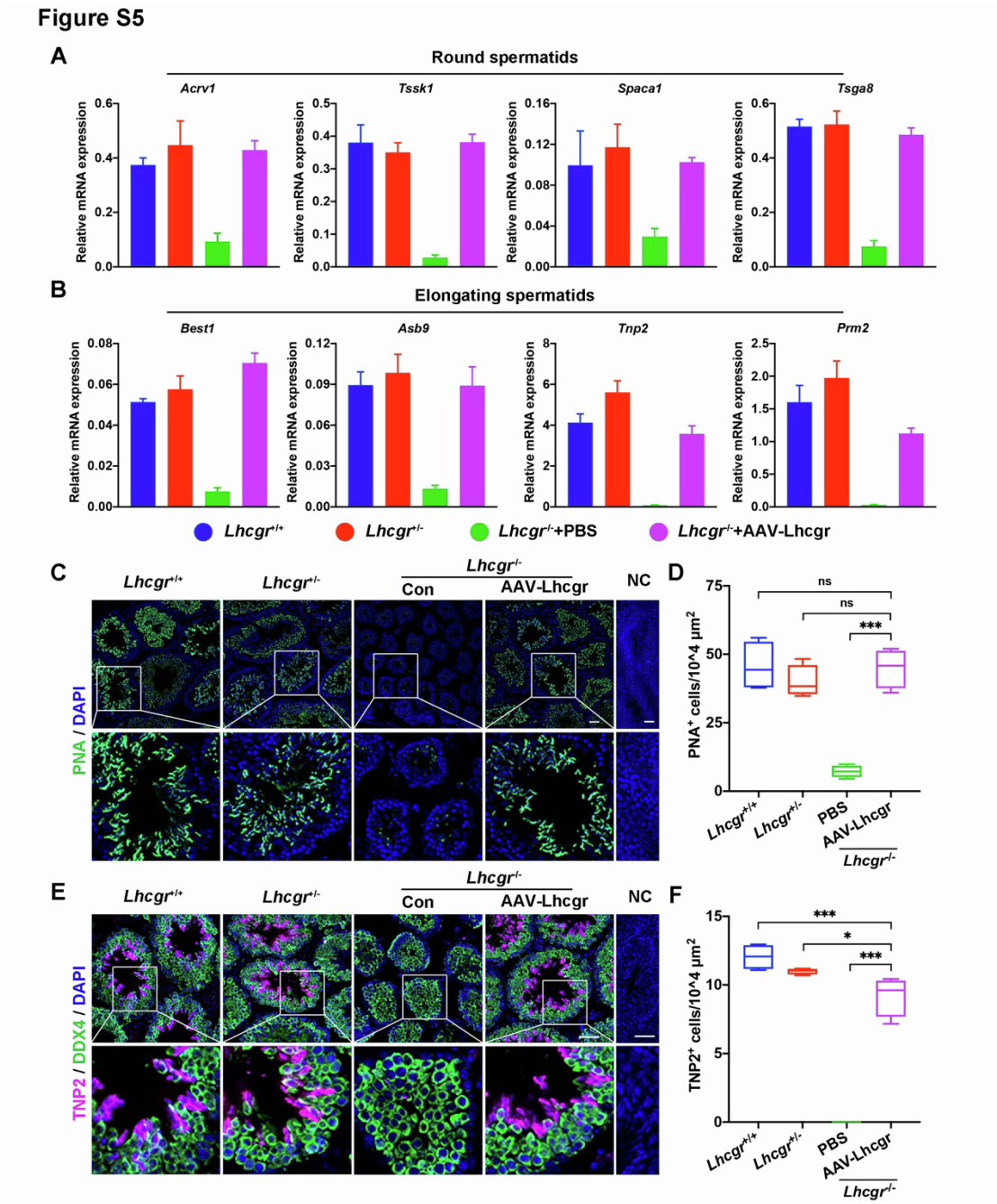

Figure S5. AAV8-Lhcgr promotes the formation of elongating spermatids in 8-week-old adult *Lhcgr*$^{-/-}$ mice. Related to Figure 7.

(A and B) Quantitative RT-PCR was used to analyze marker expression in testes samples collected from *Lhcgr*$^{+/+}$ mice, *Lhcgr*$^{+/-}$ mice, and *Lhcgr*$^{-/-}$ mice injected with PBS or AAV8-Lhcgr 4 weeks after treatment (n=3). The expression levels of marker genes for round spermatids (*Acrv1*, *Tssk1*, *Spaca1*, and *Tsga8*) and elongating spermatids (*Best1*, *Asb9*, *Tnp2*, and *Prm2*) were detected for each group. Data are expressed as mean ± sem. (C-F) Representative images of testis sections from *Lhcgr*$^{+/+}$ mice, *Lhcgr*$^{+/-}$ mice, and *Lhcgr*$^{-/-}$ mice injected with PBS or AAV8-Lhcgr (n=4). Sections were immunostained for PNA I, DDX4 and TNP2 (E), and counterstained with DAPI. Quantitative analysis showing the percentages of PNA^{+} (D) and TNP2^{+} (F) germ cells in the seminiferous tubules of the testes. NC indicates negative control. Scale bars: 50 μm. * $p < 0.05$, *** $p < 0.001$, ns = not significant.

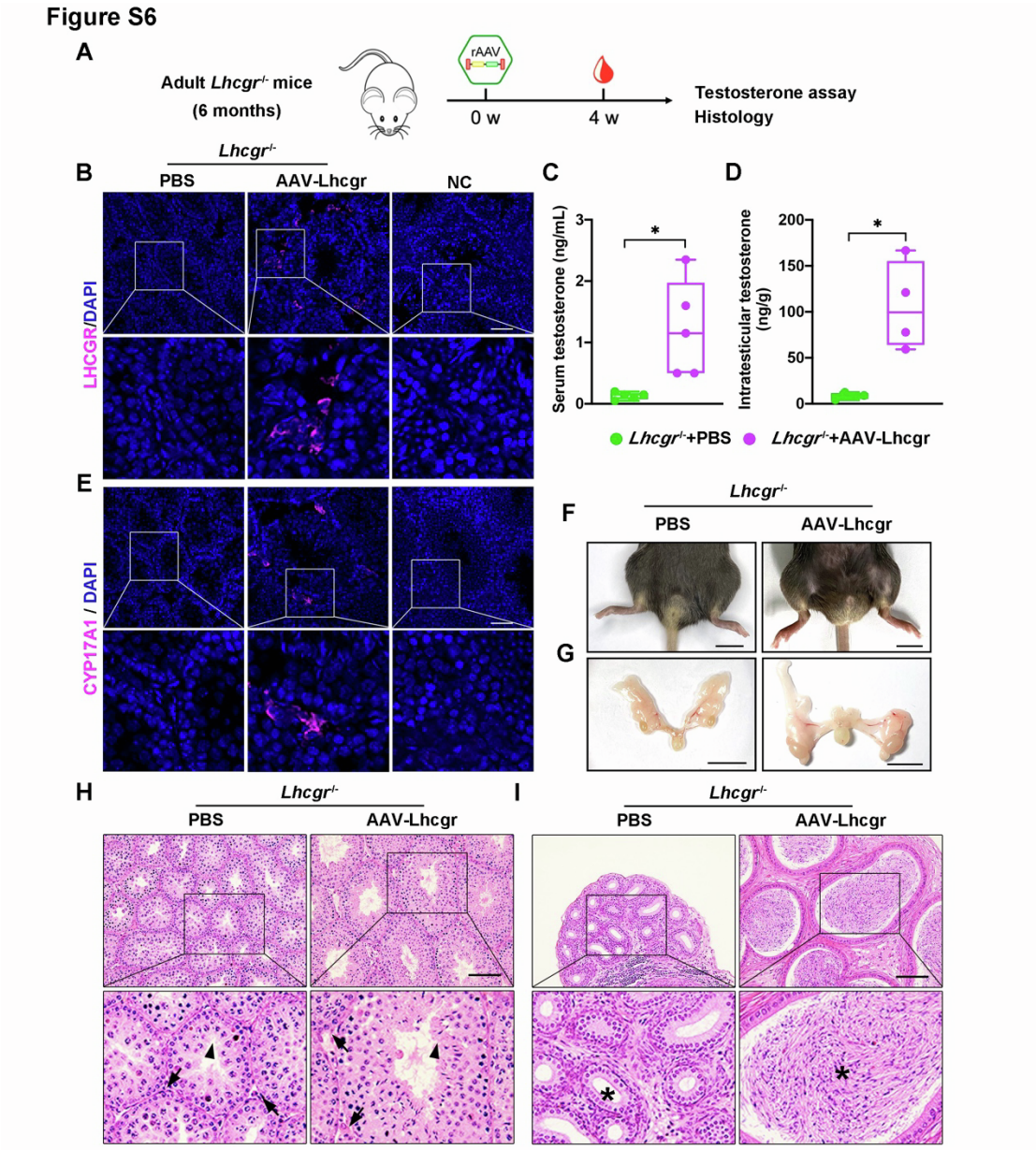

Figure S6. AAV8-Lhcgr recovers testosterone production and rescues spermatogenesis in 6-month-old adult *Lhcgr*$^{-/-}$ mice. Related to Figure 7.

(A) Experimental overview for the *in vivo* studies. (B) Representative images of LHCGR expression in the testicular interstitium at 4 weeks after treatment in 6 months *Lhcgr*$^{-/-}$ mice injected with PBS or AAV8-Lhcgr (n=4). Nuclei were counterstained with DAPI. NC indicates negative control. Scale bar: 50 µm. (C and D) The concentrations of serum (C; n=5) and intratesticular (D; n=4) testosterone were analyzed 4 weeks after treatment in 6 months old *Lhcgr*$^{-/-}$ mice injected with PBS or AAV8-Lhcgr (n=5). (E) Representative images of CYP17A1 expression in the testicular interstitium at 4 weeks after treatment in 6 months *Lhcgr*$^{-/-}$ mice injected with PBS or AAV8-Lhcgr (n=4). Nuclei were counterstained with DAPI. NC indicates negative control. Scale bar: 50 µm. (F and G) Representative photographs of external (F) and internal genitalia (G) of 6 months *Lhcgr*$^{-/-}$ mice injected with PBS or AAV8-Lhcgr (n=4) at 4 weeks after treatment. Scale bar: 1 cm. (H and I) Representative light micrographs of testes sections (H) and cauda epididymis (I) from *Lhcgr*$^{-/-}$ mice injected with PBS or AAV8-Lhcgr (n=4). Samples were taken 4 weeks after treatment. Arrows indicates Leydig cells and

arrowheads indicates full spermatogenesis in testis (H). Stars indicates spermatozoa in the cauda epididymis (I). Scale bars: 100 μm. Data are represented by box plots, and whiskers are minimum to maximum values. * $p < 0.05$.

Figure S7

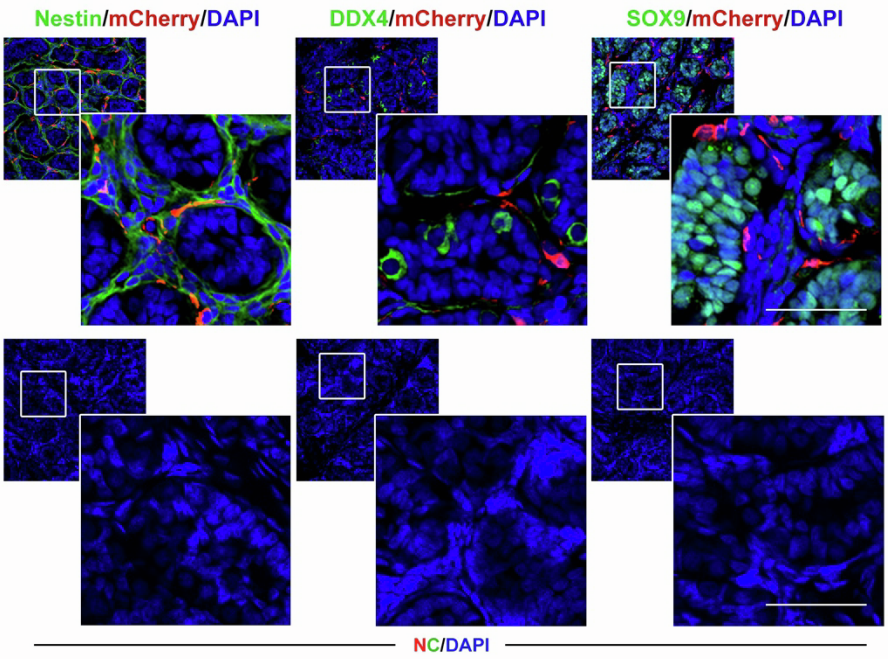

Figure S7. Testicularly injected AAV8 targets progenitor Leydig cells in non-human primates. Related to Figure 7.

Representative confocal images of the testicular sections of pubertal male cynomolgus monkeys injected with AAV8-CAG-mCherry (n=2). The testicular tissues were collected and immunostained with progenitor Leydig cells markers (Nestin), germ cell marker (DDX4), and Sertoli cell marker (SOX9) at 7 days after injection. Nuclei were counterstained with DAPI. NC indicates negative control. Scale bar: 50 μm.

Table S1. Development of embryos generated via IVF with sperm from AAV-Lhcgr-treated *Lhcgr*-/- mice in pubertal cohort. Related to Figure 5.

Lhcgr$^{-/-}$ male mice	No. of oocytes	No. of 2-cell (%)	No. of embryos transferred	No. of pseudo-pregnant mice	No. of pups (%)
M03	139	59 (42.4%)	40	2	20 (50%)
	79	31 (39.2%)	31	2	3 (9.6%)
M18	144	18 (12.5%)	18	1	10 (55.6%)
	361	70 (19.4%)	60	3	25 (41.7%)

Table S2. Primers used to amplify the transcripts in PCR analysis. Related to Star methods.

Primers for Quantitative RT-PCR

Gene	Forward Primer	Reverse Primer
Lhcgr	CACTCTCCAGAGTTGTCAGGG	GAGGTTTGTAAAAGCACCGGG
Dazl	CTTCATCAGCAACCACAA	TTCATCCATCCTAACATCAAT
Uchl1	TGGAATTTGAGGATGGAT	AACACTTGGCTCTATCTT
Sycp3	CGCTGAGCAAACATCTAAAGA	CAACCAAAGGTGGCTTCC
Tex101	TACCTTTAACTGGACTTCA	CCATCTGCTTTAATCAACA
Acrv1	CAGGTGAACAGGTGTCTA	CAGATGTGCTTGGAAGTG
Tssk1	CAAGGACTTCAACATCAA	GGTCTTGCTTAATATCAGT
Spaca1	ATTCACCGTCTATACAAC	CAGATAATGACTCCTATGG
Tsga8	GTGAAGCCTATAATGCCAAT	ACCCTTTCCACAAAGAATG
Asb9	ACTATAACATCAGCCATC	CCTTGATTCACAGATACT
Best1	AACTTGAACATTCCAGAG	TCATTAGAGCCTGTATATTG
Prm2	GGACTATGGGAGGACACA	ATCCTATGTAGCCTCTTACGA

Tnp2	AAAGTGAGCAAGAGAAAGG	TTGTATCTTCGCCCTGAG
Il1β	TGGACCTTCCAGGATGAGGACA	GTTCATCTCGGAGCCTGTAGTG
Il6	TAGTCCTTCCTACCCCAATTTCC	TTGGTCCTTAGCCACTCCTTC
Ifnb1	CAGCTCCAAGAAAGGACGAAC	GGCAGTGTAACTCTTCTGCAT
Ifna13	AGGATGTGACCTGCCTCAGACT	CACCTTCTCCTGTGGGAATCCA
Primers for Genotyping		
Lhcgr wild type	TGACCTGTTCCTGGGGCTGCTG	AAATGGCCTCAACGGGTGTGCA
Lhcgr mutant type	ATGGGATCGGCCATTGAACAAG	TCAGAAGAACTCGTCAAGAAGGC
Primers for Integration Assay		
Lhcgr	AGCTAATGCCTTTGACAACCTC	CGAGATTAGCGTCGTCCCAT
CAG	TTCGGCTTCTGGCGTGTGA	GGTGAGAGATAGTCGGGCG
Primers for Probe Synthesis		
AAV vector	TCCTGTCCCCTCAGTTCA	AATTGCATTCATTTTATGTTTC